Aalto University
School of Chemical
Engineering

Emmi-Maria Nuutinen

FEATHER CHARACTERIZATION AND PROCESSING

Master´s Programme in Chemical, Biochemical and Materials Engineering
Major in Fibre and Polymer Engineering

Master's thesis for the degree of Master of Science in Technology submitted for inspection, Espoo, 4th September, 2017.

Supervisor Professor Tapani Vuorinen

Instructor D. Sc. Anna-Stiina Jääskeläinen

Aalto University
School of Chemical
Engineering

Aalto University, P.O. BOX 11000, 00076 AALTO
www.aalto.fi

Abstract of master's thesis

Author	Emmi-Maria Nuutinen
Title of thesis	Feather characterization and processing
Degree Programme	Chemical, Biochemical and Materials Engineering
Major	Fibre and Polymer Engineering
Thesis supervisor	Professor Tapani Vuorinen
Thesis advisor(s) / Thesis examiner(s)	D. Sc. Anna-Stiina Jääskeläinen
Date 04.09.2017	**Number of pages** 69+7 **Language** English

Abstract

The aim of this thesis was to revise the existing knowledge of the complex hierarchical structure of the feathers and validate the selected analytical methods for the native and processed feather characterization.

The rachis in which the barbs are attached were separated from each other, and these structural parts of the native feathers were characterized separately. The processed feathers were obtained by steam explosion and deep eutectic solvent (DES) fractionation. All the feather samples were characterized using various techniques, and the focus was especially on the characterization of the secondary structures. The applied methods were: optical microscopy, elemental analysis, amino acid analysis, attenuated total reflectance Fourier transform infrared spectroscopy (ATR-FTIR), Raman spectroscopy, X-ray diffraction crystallography (XRD), and solid state nuclear magnetic resonance spectroscopy (NMR).

In the characterization process, it was observed the feathers consist almost entirely of keratin. Moreover, the rachis and barbs consist of the fibre like outer layer and the inner honeycomb structure. In the outer layers, the polypeptide chains are axially oriented while in the inner honeycomb structure, they have a larger range of conformations and orientations. It was also observed that the rachis contains more secondary structure β-sheet and has a higher degree of crystallinity compared to the barbs. In turn, the content of fat is higher in the barbs. It is suggested that in the feather structure, rachis provides the structural support while barbs form the protective outer layer.

After processing, both, the chemical composition and structure of the feathers were changed, and the different method had a different effect. This means that by varying the processing method and conditions, different macro properties for the end product can be obtained.

Based on the valuable information provided by the different characterization methods, Raman spectroscopy showed a great potential in the characterization of the native feathers while optical microscopy, ATR-FTIR, and XRD were beneficial and informative in the characterization of both, native and processed feathers.

Keywords Feather, keratin, characterization, processing, secondary structure

Aalto-yliopisto
Kemian tekniikan korkeakoulu

Aalto-yliopisto, PL 11000, 00076 AALTO
www.aalto.fi

Diplomityön tiivistelmä

Tekijä Emmi-Maria Nuutinen

Työn nimi Höyhen karakterisointi ja prosessointi

Koulutusohjelma Chemical, Biochemical and Materials Engineering

Pääaine Fibre and Polymer Engineering

Työn valvoja Professori Tapani Vuorinen

Työn ohjaaja(t)/Työn tarkastaja(t) TkT Anna-Stiina Jääskeläinen

Päivämäärä 04.09.2017 **Sivumäärä** 69+7 **Kieli** englanti

Tiivistelmä

Tämän diplomityön tarkoituksena oli tarkistaa ja päivittää nykyinen tietämys höyhenen monimutkaisesta ja hierarkkisesta rakenteesta sekä validoida menetelmät alkuperäisen ja prosessoidun höyhenen karakterisointiin.

Ruoto ja siinä kiinni olevat höytyliistakkeet erotettiin toisistaan ja nämä rakenteelliset osat karakterisointiin erikseen. Höyheniä prosessoitiin höyryräjäytyksellä sekä liuottamalla höyhenet eutektiseen liuottimeen. Kaikki höyhennäytteet karakterisoitiin eri tekniikoilla, keskittyen erityisesti sekundäärirakenteen karakterisointiin. Tässä työssä käytetyt menetelmät olivat: optinen mikroskopia, alkuaineanalyysi, aminohappoanalyysi, heikentynyt kokonaisheijastus Fourier-muunnosinfrapunaspektroskopia (ATR-FTIR), Raman-spektroskopia, röntgenkristallografia (XRD) sekä kiinteäntilan ydinmagneettinen resonanssispektroskopia (NMR).

Karakterisointiprosessi osoitti, että höyhenet koostuvat melkein kokonaan keratiinista. Lisäksi huomattiin, että ruoto ja höytyliistakkeet koostuvat kuitumaisesta ulkokuoresta sekä hunajakennomaisesta sisärakenteesta. Ulkokuoren polypeptidiketjut huomattiin olevan aksiaalisesti suuntautuneita, kun taas hunajakennorakenteessa niillä ei huomattu olevan selkeää suuntautumista. Alkuperäisen höyhenen karakterisoinnissa havaittiin myös, että ruoto-osassa on enemmän β-laskosta ja korkeampi kiteisyysaste kuin höytyliistakkeissa. Toisaalta, höytyliistakkeissa huomattiin olevan enemmän rasvaa. Tulosten perusteella voidaan olettaa, että höyhenessä ruoto-osan tehtävä on antaa rakenteellista tukea, kun taas höytyliistakkeiden tehtävä on muodostaa suojaava ulkokerros.

Prosessoinnin jälkeen höyhenkeratiinin kemiallinen koostumus sekä rakenne olivat muuttuneet. Huomattiin myös, että eri prosessointimenetelmällä oli erilainen vaikutus. Tämä tarkoittaa, että vaihtelemalla prosessointimenetelmää sekä -olosuhteita, lopputuotteelle voidaan optimoida erilaiset makro-ominaisuudet.

Perustuen eri karakterisointimenetelmien antamaan tietoon voidaan todeta, että Raman-spektroskopia oli hyvä karakterisointimenetelmä alkuperäiselle höyhenelle, kun taas optinen mikroskopia, ATR-FTIR sekä XRD olivat hyödyllisiä niin alkuperäisen kuin prosessoidunkin höyhenen karakterisoinnissa.

Avainsanat Höyhen, keratiini, karakterisointi, prosessointi, sekundäärirakenne

Preface

The research was carried out at VTT Technical Research Centre of Finland in Espoo during the time period of February to August 2017.

I would like to thank my thesis supervisor Professor Tapani Vuorinen for his advice and support. I also want to thank my instructor Anna-Stiina Jääskeläinen for providing me the opportunity for this thesis and for her instruction. Thank you for all the guidance during the thesis and for interesting discussions which helped me to deepen my understanding.

Furthermore, I am thankful to all the people at VTT who made me feel welcomed and helped me to use the devices. Thank you for the discussions which helped me to achieve my goal.

I want also thank Alice Mija for giving me the opportunity to travel to Nice and carry out my measurements in the University of Nice Sophia Antipolis. Thank you for making me feel welcomed and for the discussions.

Finally, I want to thank my family and friends for all the support during my studies.

Espoo, September 4th, 2017
Emmi-Maria Nuutinen

Table of Contents

APPENDICES

List of abbreviations

Ala	alanine
Arg	arginine
Asp	aspartic acid
ATR	attenuated total reflectance
C	carbon
CD	circular dichroism
Cys	cysteine
DES	deep eutectic solvent
FTIR	Fourier transform infrared spectroscopy
Glu	glutamic acid
Gly	glycine
H	hydrogen
His	histidine
HPLC	high-pressure liquid chromatography
IL	ionic liquid
Ile	isoleucine
Leu	leucine
Lys	lysine
Met	methionine
N	nitrogen
NMR	nuclear magnetic resonance spectroscopy
O	oxygen
Phe	phenylalanine
Pro	proline
S	sulphur
Ser	serine
SFE	stem flash explosion
Thr	threonine
Tyr	tyrosine
Val	valine
wt%	weight percent
XRD	X-ray diffraction crystallography

1. Introduction

Today, people are more aware of the environmental issues and their relations to petroleum based products than ever before. Legislative policies are forcing industries and companies to find renewable resources to replace the conventional ones. This has driven us closer and closer to natural resources and their utilization. However, while the demand for environmentally responsible applications is increasing, the concern about the scarcity and accessibility of natural resources is raised. At the same time, the growth of population, increasing urbanization and higher standards of living generate more and more waste all the time. This waste also includes bio-based materials which could be further utilized. This is why, recently, researchers and industries are focusing on to find new ways to utilize bio-based waste streams in order to develop value added renewable and sustainable product solutions to replace conventional ones.

When considering the most globally abundant, unique and inexpensive waste streams which could be utilized for value added applications, one cannot pass poultry industry. The waste stream in poultry industry consists of feathers, internal organs, blood, bones, skin, feet and residual meat. From these coproducts, especially, poultry feathers have attracted interest. It has been predicted that in 2017, only the broiler meat production will be 89.5 million tons worldwide (USDA, 2017). If it is then assumed that the poultry industry waste covers 30 % of its total weight (Jamdar & Harikumar, 2005), and chicken feathers constitute approximately 10 % of chicken's weight (Grazziotin et al., 2007), the chicken feather waste can be assumed to be 12 million tons worldwide. At the moment, these feathers are mainly disposed in landfills or used as low-value animal feed. However, these feathers could also provide a possibility to be further converted, for example, into fibers, films, hydrogels, nano and micro particles which could be then utilized in industries such as food, cosmetology, agriculture, textile, composite and medical industries. (Reddy, 2015)

Feathers are considered as the most complex integumentary appendages on vertebrates (McKittrick et al., 2012). Their main function in chickens as tough, durable, insoluble, fibrous material is to provide outer protection layer (Schrooyen et al., 2001) as well as temperature control, mechanical strength and elasticity (Martinez-Hernandez et al., 2005). In general, feathers have low density, a hollow honeycomb structure, unique hierarchical architecture and they are biodegradable and consist approximately 90 % of a protein called keratin which is mostly responsible for their

properties (Reddy, 2015). Moreover, feathers, as well as other keratin rich natural materials, are considered as a composite like material in which highly oriented keratin microfibrils are embedded in an amorphous keratin matrix (Feughelman, 2002; Filshie, 1962; Martinez-Hernandez et al., 2005; McKittrick et al., 2012). These unique properties combined with the abundant availability and low cost make feathers a potential choice for various applications in which properties like high tensile strength and elasticity are desirable.

At the moment, feathers are not utilized in high-value applications at a larger scale (Reddy, 2015). In order to realize the full potential of the feathers and their suitability and behavior for different processes and applications, a deeper understanding of the relation between the hierarchical structure and the functional protein properties is necessary. Especially, understanding the dependence of the macro properties to the structures and dynamics at a molecular level is important in order to understand the functional design of biomaterials (Duer et al., 2003). This thesis will start with literature review in which the structure of the chicken feather will be presented generally. This will be followed by the introduction to characterization methods which have been applied for feathers. Also, some processing techniques will be discussed. The literature review will be then followed by the experimental part which will include broad characterization of chicken feathers, especially focusing on the secondary structure of the keratin. Also, two sorts of environmentally friendly processing methods will be applied for the feathers: steam explosion and extraction with deep eutectic solvents. Characterization of these processed feathers and regenerated keratin will be also included in this thesis. The aim of the work is to revise the existing knowledge of the feather's complex hierarchical structure and validate the selected analytical methods for feather characterization. Furthermore, the changes in the feather's structure caused by the processing and regeneration will be identified, and the best characterization methods for that will be identified.

2. Structure of the feather

Chicken feathers are a complex and branched structure resulted from the biological evolution (Xu et al., 2001) and they cover approximately 10 % of the chicken's weight (Grazziotin et al., 2007). In general, they consist of three main units called rachis also known as quill, barbs and barbules (Figure 1). The barbules are considered as the tertiary structures which are attaches to the secondary structures, barbs. Barbs are then attached to the rachis which is the primary structure of the feather. The rachis

can have a length up to 18 cm while the barbs can be anywhere from 1 to 4.5 cm. The barbules have a hook-like structure and the length of 0.3-0.5 mm. (Reddy & Yang, 2007) Both, rachises and barbs, have been noticed to have an inner honeycomb structure which enables the low weight and density of the feathers (Huda & Yang, 2008; Reddy & Yang, 2007). Furthermore, the rachis covers approximately 50 % of the weight of the chicken feathers while the other half is usually considered as feather fiber (including barbs and barbules) (Winandy et al., 2003).

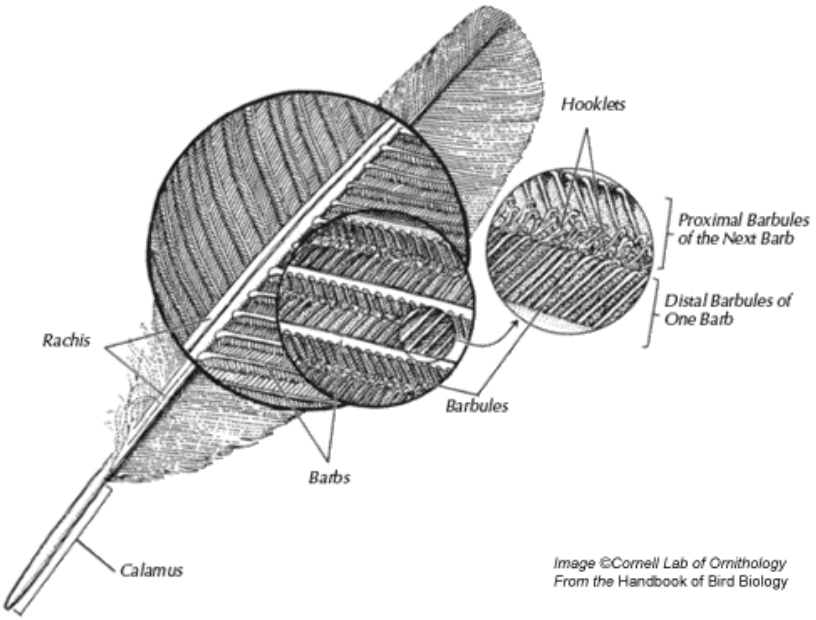

Figure 1. The schematic representation of the feather's hierarchical and branched structure.

Feathers consist approximately of 91% protein called keratin, 1% fat and 8% water (Chinta et al. 2013). After collagen, keratin is considered as the most important structural bio polymer found in animals. The natural materials which consist mainly of keratin can be called as keratinized materials. Besides the chicken and other bird feathers, for example, hooves, horns, nails, wool, and the epidermal layer of the skin are rich in keratin. Keratin in mammals is called α-keratin while in reptiles and birds keratin is called β-keratin which is tougher than α-keratin. In general, β-keratin is rich in β-sheets while α-keratin is rich in α-helices. All the keratinized materials have then a variety of morphologies depending on their function. For example, horn is a strong, impact resistance material while turtle shell's main function is to provide the waterproof layer. For feathers, the main functions are flight, camouflage, courtship, thermal insulation and water resistance. (McKittrick et al., 2012)

All the keratinized materials can be considered as keratin fiber reinforced composites which consist of crystalline highly axially oriented intermediate filaments (microfibrils) embedded in an amorphous, non-fibrous, protein matrix (Feughelman, 2002; Filshie, 1962; Martinez-Hernandez et al., 2005; McKittrick et al., 2012). The protein matrix is assumed to compose of globular proteins and water (Feughelman, 2002). It has been suggested that the complex filamentous hierarchy provides, for example, the high toughness of the chicken feather's rachis. However, the study of this structure is difficult due to the tight bonding between the filaments and the matrix. (Lingham-Soliar et al., 2010) Nevertheless, some attempts have been carried out in order to study this hierarchy already in 1962 by Filshie (1962). Also, Lingham-Soliar et al. (2010) have developed their own interpretations of the fine structure of the feather's rachis (Figure 2).

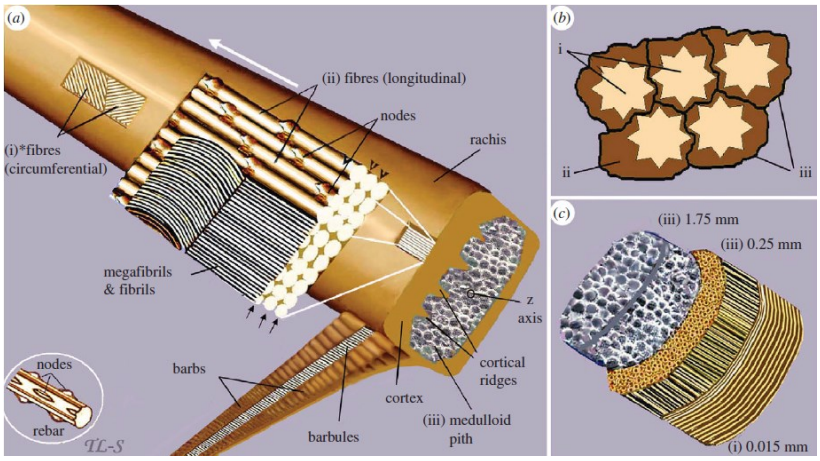

Figure 2. The schematic illustration of the fine structure of the feather presented by Lingham-Soliar et al. (2010): the keratin fibers and the filamentous hierarchy (a), the cross section of fibers embedded in the amorphous protein matrix (b), and the three-dimensional cross section showing the thicknesses (c).

Keratin is a fibrous structural protein (Feughelman, 2002; Filshie, 1962; Lingham-Soliar et al., 2010; Pauling & Corey, 1943; Rintoul et al., 2000; Schor & Krimm, 1961; Schrooyen et al., 2000) which is mechanically efficient in both, tension and compression (Lingham-Soliar et al., 2010; McKittrick et al., 2012). Generally, fibrous proteins have a period amino acid sequence and highly ordered structure (Yoshimizu et al., 1991) whose shape is dominated by a secondary structure (Voet & Voet 2004). Like all proteins, also, fibrous keratin consists of biological polymers, polypeptide chains. These polypeptide chains consist of amino acid residues and are resulted from the condensation of amino acids. (Feughelman, 2002) The peptide bond is

formed when carboxyl group of one amino acid reacts with the amino group of another amino acid. It has been suggested that one feather keratin microfibril consists approximately of 15-21 polypeptide chains (Filshie, 1962), and one polypeptide chain contains about 96 amino acid residues (Arai 1983) from which Serine (Ser), proline (Pro), Glycine (Gly), Valine (Val), Cysteine (Cys), and Leucine (Leu) are usually the most abundant ones (Schmidt & Jayasundera, 2003). It has to be noted that the amino acid content of different feathers can vary a lot, for example, due to breed, feed and environment (Martinez-Hernandez et al., 2005). It is also important to notice that even same keratin source can contain different types of polypeptide chains depending, for example, on location in the feather structure (Alger, 1996).

The feather keratin poses two different ordered conformation in its secondary structure. The polypeptide chain can be either curl into alpha helix or bond into plated sheets, β-sheets (Figure 3) (McKittrick et al., 2012). The ratio of these conformations depends on the location of the polypeptide chain. In general, it has been suggested that barbs and barbules consist slightly more of α-helices than β-sheets while the outer rachis is rather richer in β-sheets (Schmidt & Jayasundera, 2003). Besides the ordered structure, the feather keratin includes some disordered structure (random coil) (Schmidt & Jayasundera, 2003), and chain reversal regions called β-turns between the β-sheets (Chou & Fasman, 1978). Intramolecular bonding within the protein backbone is responsible for the secondary structure while the tertiary structure (the three-dimensional shape) is due to intermolecular bonding between the side groups and spatial arrangements of the secondary structure (Alberts et al., 1994).

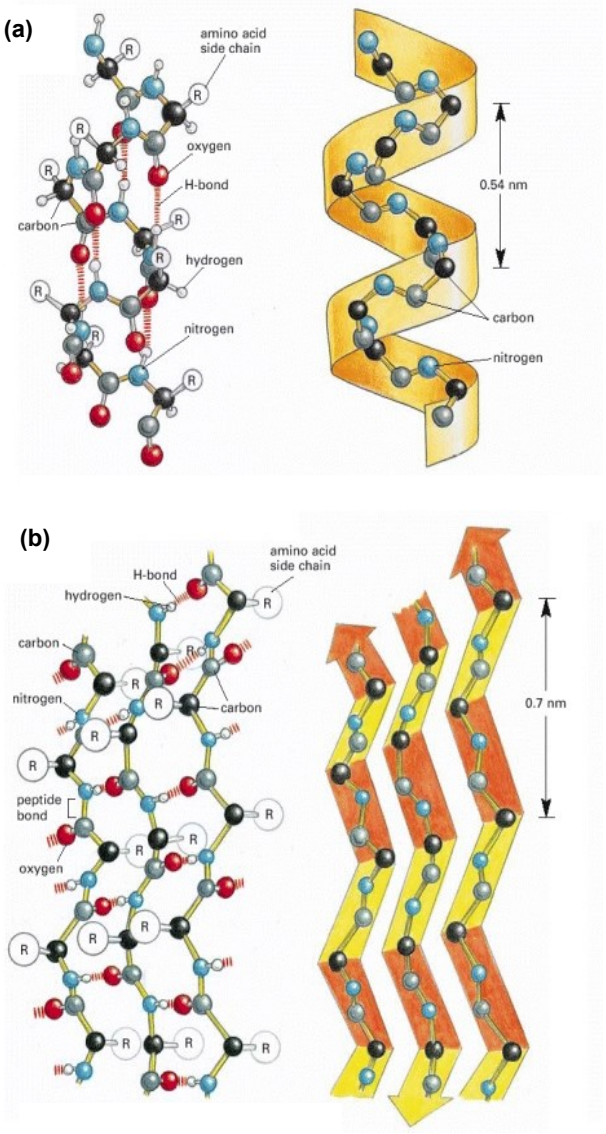

Figure 3. The schematic illustration of the secondary structures: α-helix (a) and antiparallel β-sheet (b) (figure is modified from the source: Alberts et al., 1994).

Keratin fiber is relatively rich in cysteine residues which are partly responsible for the great stability of feather keratin. Cysteine has sulfhydryl (SH) groups which are able to form a network by crosslinking adjacent polypeptide chains via sulphur-sulphur covalent bonds (disulfide bonding) (Figure 4). (Martinez-Hernandez et al., 2005; Saravanan & Dhurai, 2012) These disulfide bonds between cysteine residues play an important role in stabilizing the protein folded structure and the association with the other polypeptide chains (Alberts et al., 1994). In keratinized materials, disulfide bonding takes also place between the matrix and crystalline fibers. The hardness of the keratin rich material depends strongly on this disulfide bonding. For example, skin

is considered as soft keratin as it does not contain as much thiol groups as, for example, hooves. (McKittrick et al., 2012) In feathers, the covalent disulfide bonding is suggested to protect them against environmental degradation by heat, cold, light, water, biological attack and mechanical distortion (Feughelman, 2002).

Besides the covalent bonding, there is a range of non-covalent interactions present in the keratin fiber such as Van der Waals forces, hydrogen, ionic and hydrophobic bonds (Feughelman, 2002; Martinez-Hernandez et al., 2005). For example, both the -NH and -C=O groups enable the formation of the inter and intra chain hydrogen bonds while the side chains can form electrostatic, polar and hydrophobic interactions as well as hydrogen bonds between the polypeptide chains (Feughelman, 2002). Moreover, the polypeptide chain of keratin protein include both hydrophilic and hydrophobic amino acids, and these amino acids can be either internal or external to the surface. Thus, the surface properties of the keratin fiber depend mostly on the degree of the internal and external amino acids (Schmidt & Jayasundera, 2003).

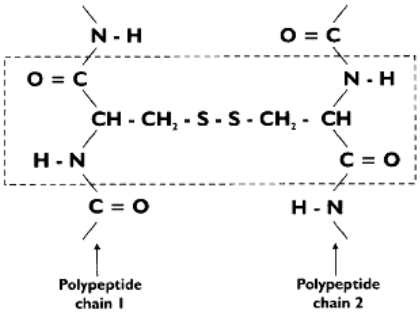

Figure 4. Diagrammatic illustration of the cysteine residue linking two polypeptide chains forming cystine (Feughelman, 2002).

3. Characterization methods for feathers

Feathers are considered to be the most complex evolutionary integumentary appendages with structural diversity and hierarchical development (Prum, 1999). And as already mentioned, the study of the feather structures is difficult due to tight bonding between the keratin fibers and matrix (Lingham-Soliar et al., 2010). It is also important to keep in mind that the different parts in the feather structure (calamus, rachis, and barbs) may have different chemical composition and structure as well as different physiochemical properties. However, in order to be able to process and utilize feathers as efficient as possible, the understanding of the feather structures is necessary. Also, to realize and understand the changes during and after the

processing is critical. To discover and recognize the complex feather structure, different characterization methods have been applied, and some of these techniques will be presented in this chapter. These techniques have been used to characterize the unmodified feathers as well as processed, regenerated and modified feathers.

3.1 Chemical composition and structure

From the chemical viewpoint, proteins are known to be the most structurally complex and functionally advanced molecules (Alberts et al., 1994). The study of the chemical composition and structure of the protein covers the study from its elemental composition to its spatial arrangement and bonds holding the structures together. It is clear that the chemical composition and structure as well as the interactions determine the behavior and properties of the protein. This is why their characterization is essential in order to achieve a better understanding of the feather keratin. In this section, some of these characterization techniques will be presented. At the moment, not much is known about the conformation of the polypeptide chain in β-keratins or the correlation between their filamentous structure and properties (Fraser & Parry, 2011). However, feather keratin is considered to be a fibrous protein (vs. globular) which means that the protein structure results from a relative homogenous secondary structures formed of repetitive primary sequences (Wang et al., 2006). This is why in this Master's thesis, the characterization of the secondary structures is especially taken into account. Another interesting research area would be studying the intra and intermolecular bonding present in feather, for example, the bonding between the matrix and microfibrils.

3.1.1 Elemental composition

By knowing the content of different elements in feather keratin can give us valuable information in understanding the chemical composition and structure of the protein rich biologicals material. Especially, interesting is the determination of sulphur (S) nitrogen (N) contents. The content of S can be used to predict the disulfide crosslinking while the content of N can be used to determine the protein content in the feather keratin.

For feathers, the elemental analysis is mostly carried out by CHNS elemental analyzer (Aguayo-Villarreal et al., 2011; Kammiovirta et al., 2016; Sun et al., 2009; Tuna et al., 2015; Yin et al., 2013). CHNS elemental analyzer is considered as a rapid method which determines carbon (C), hydrogen (H), nitrogen (N) and sulphur (S) portion in materials, and it is usually used for organic materials. In general, CHNS

analysis uses a combustion process to break down the sample into simpler compounds (combustion products) which are then detected. The combustion process is carried out at high temperature. In order to carry out the analysis successfully, some considerations have to be taken into account. First of all, the sample should be as homogeneous as possible in order to achieve reliable results. Also, the formation and removal of ash during the combustion process can cause issues. Despite these considerations, CHNS analysis is considered as a relatively reliable method (Thompson, 2008).

As already mentioned, the elemental analysis has been successfully carried out for chicken feathers. Aguayo-Villarreal et al. (2011) used elemental analysis to determine the elemental composition of the feather's barbs and evaluate their possible usage as sorbents. Yin et al. (2013) used elemental analysis to support and supplement the results from the amino acid analysis, especially the sulphur content was taken under investigation. In the study of Kammiovirta et al. (2016) was used to determine the protein content. Also, Tuna et al. (2015) studied the elemental composition of feathers. In their studies, different color feathers were compared by their elemental composition, and the elemental analysis was carried out before and after pyrolysis. Especially, the C/N ratio was under investigation. This ratio was used to interpret, for example, the occurred degradation after pyrolysis (Tuna et al., 2015). As will be appreciated, the elemental analysis itself cannot predict the secondary structure of the feather keratin. Nevertheless, as a rapid and simple method it could be a good technique to characterize the changes that take place during the processing, regeneration or modification. This, however, requires defining the correlations between the elemental analysis and other characterization methods so the changes can be interpreted.

3.1.2 Amino acid content

To understand the chemical composition of the keratin molecule, amino acid analyses play an important role. Especially, the characterization of the cysteine content is interesting as it is responsible for the disulfide bonding, and this way for more stable folded structure. By knowing the amino acid composition, also, some intra and interactions can be predicted.

In comparison to elemental analysis, amino acid composition is more common characterization method for feathers. It has been stated that the amino acid content determines the shape of the protein (Alberts et al. 1994), and this why it could also

be used to predict the secondary structure of the protein (Chou, P. Y., & Fasman, G. D. (1974)). Proteins consist of amino acid residues linked to each other by covalent bonding forming an organized and folded polymer, polypeptide, chain. When the amino acid content is determined, protein is hydrolyzed into its individual amino acid constituents. Usually, this is done by acid hydrolysis. The hydrolyzed amino acids are then chromatographically separated and quantified, usually using a high-pressure liquid chromatography (HPLC). In order to obtain accurate results, the sample should be as purified as possible. Furthermore, acid hydrolysis can cause a complete or partial destruction of selected amino acids. This, on the other hand, will cause a variation and error to the analysis. (Anonymous, 2005) This is also why Yin et al. (2013) used elemental analysis to correct the inadequate cysteine residue resulted from the amino acid analysis.

The amino acid composition of the feather keratin has already been studied in 1964 by Harrap & Woods. Nowadays, there can be found many studies in which this characterization technique has been applied for feathers including studies of Dalev (1994), Arai et al. (1983), Wang et al. (2016), Yin et al. (2013), and Zhao et al. (2012). In general, amino acid analysis can be considered as a relatively informative method. From the amino acid nature (especially the nature of the side chains) and distribution within the protein, some interpretations about the hydrophilicity and hydrophobicity as well as about the charge of the protein can be concluded. This, on the other hand, provides an opportunity to predict the bonding, (Fraser & Parry, 2008; Martinez-Hernandez et al., 2005; Shi & Dumont, 2014; Yin et al., 2013), and even the secondary structure and three-dimensional shape of the protein (Chou & Fasman, 1974). However, the destruction of some amino acids as well as the complexity and time consumption of the analysis method have to be taken into account when considering this method.

3.1.3 Acidity and basicity

As already mentioned in the previous section, by determining the amino acid content of the protein, something about its acidity and basicity could be assumed as their side groups are known (Fraser & Parry, 2008; Martinez-Hernandez et al., 2005; Shi & Dumont, 2014). Another possible way to determine the acidity and basicity of the feather samples is potentiometric titration. This has been done by Aguayo-Villarreal et al. (2011) who followed the methodology of Faria et al. (2004). In this methodology, the samples are mixed and put in contact with base (NaOH) for 48 hours. This will be followed by the decantation of the suspension, and titration of the remaining NaOH

solution with acid (HCl). With this procedure, the total acidity and charge of the sample can be determined. In order to obtain the basicity, the sample has to be put in the contact with acid, and the titration is carried out with base. (Faria et al., 2004) Also, some other titrations have been carried out in feather studies. However, in these studies, the feathers have been modified with some chemicals, and the success of the modification and the consumption of the chemicals have been determined by the titration (Hu et al., 2011; Ji et al., 2014; Reddy et al., 2011). To summarize, it can be said that the titration could be a simple method to determine the acidity and basicity especially in situations where a certain level of acidity or basicity is required for chosen specific application such as absorbents.

3.1.4 Secondary structure

Secondary structure results from the bonding within the polypeptide backbones (Alberts et al., 1994), and fibrous proteins are considered as regular secondary structures (Fraser, 2012). When secondary structures are characterized, the α-helices, β-sheets, β-turns and random coils (unordered structures) present in protein structure are identified. The secondary structure of the protein (before and after processing) has usually been characterized by spectroscopic techniques such as circular dichroism (CD), nuclear magnetic resonance spectroscopy (NMR), X-ray diffraction crystallography (XRD) and infrared spectroscopy (IR) (Goormaghtigh et al., 1990).

From these techniques IR, especially Fourier transform infrared spectroscopy (FTIR), is very commonly used to characterize the secondary structure of the raw and processed feathers (Sun et al., 2009; Yin et al., 2013; Saravanan et al., 2013; Pedram Rad et al., 2012; Ma et al., 2016; Zhao-Tie et al., 2009; Ullah & Wu, 2013; Ji et al., 2014; Hu et al., 2011; Khosa et al., 2013; Wang & Cao, 2012; Wang et al., 2016; Schmidt and Jayasundera, 2003; Tuna et al., 2015). Also, attenuated total reflectance Fourier transform infrared spectroscopy (ATR-FTIR) has used to study the chemical structure of the feather keratin (Aguayo-Villarreal et al., 2011; Kammiovirta et al., 2016; Yin et al., 2013; Zhang et al., 2015). FTIR has a great potential when substances have to be identified and quantified. The technique is based on the molecular vibrations in the sample. Molecules in the specific bonds absorb infrared light characteristically based on their structure and chemical environment (i.e. the intra and intermolecular bonding). The absorption spectrum is obtained by passing infrared radiation through the sample, and by determining the absorbed radiation. The

formed characteristic spectrum then allows the identification. In this technique, the sample can be in the form of solid, liquid or gas. (Stuart, 2003)

ATR-FTIR differs from FTIR only by the way sample is measured. In FTIR, solid sample is usually pressed to KBr-pellet while in ATR-FTIR, solid sample does not require any pretreatment. The phenomena in ATR-FTIR is based on the total internal reflection. The beam of radiation enters a crystal on which the sample is located and undergoes total reflection. The sample is in close contact with the crystal allowing the infrared beam to penetrate in the sample which then selectively absorb the radiation. The beam loses energy, and the absorption spectrum can be detected. Because the beam does not transmit the sample but rather touches the surface, the strong disturbing IR signals, such as the signals from aqueous solutions, can be avoided. This makes it more suitable also for bulk samples. ATR-FTIR is suitable for both, solid and liquid, samples. (Stuart, 2003)

There are lots of literature available in order to identify the arisen characteristic absorption bands in proteins. In chicken feathers, the adsorption bands are mainly due to peptide bonds (-CHNO-). The vibrations in these peptide bonds can be then used to assess the secondary structure (Barth, 2007; Miyazawa & Blout, 1961). FTIR has also been used to determine the changes in the secondary structure after processing such as unfolding (Hu et al., 2011) or reduction of β-sheet structure (Kammiovirta et al., 2016; Khosa et al., 2013). Additionally, the secondary structure has been used to interpret the crystallinity (Pedram Rad et al., 2012), and the destruction and changes of the disulfide bonding have been interpreted (Saravanan et al., 2013; Wang et al., 2016). One example of the possible FTIR spectrum for feather keratin is shown in Figure 5.

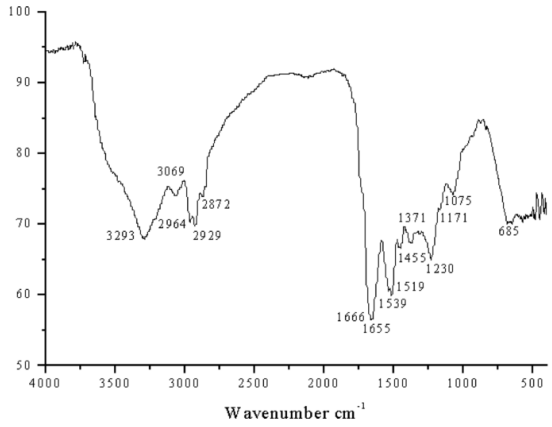

Figure 5. FTIR spectrum for feather keratin (Martinez-Hernandez et al., 2005).

Like IR also Raman spectroscopy is based on the molecular vibrations. When light interact with the matter, the photons can either absorb or scatter from it. While IR is based on the absorption, Raman spectra are based on the scattering. The scattered light has a different energy than the incident light. This energy can be then used to determine the wavenumber of the scattered light, and the spectra are presented in the form of intensity of scattered light versus wavenumber. (Smith & Dent, 2005) Moreover, the laser beam is used to excite the Raman scattering (Ferraro & Nakamoto, 2003; Smith & Dent, 2005). With Raman spectroscopy, some problems related to fluorescence and degradation can occur. These problems, however, have been reduced with advanced technology. The Raman sensitivity can be improved by using the highest frequency as possible. This usually means the use of ultraviolet (UV) region. Moreover, usually, when spectra are measured and the excitation of the scattering takes place in the UV region, less fluorescence is observed. However, because the UV photons have relatively high energy, higher risk of sample burning is present. (Smith & Dent, 2005) UV Raman also requires samples to be as flat and homogenous as possible which is difficult in the case of feather samples. With the UV Raman, the spectrum is usually measured as an average from rotating sample while the visible light Raman can enable very accurate choice of the measurement point with the help of optical microscopy (Jääskeläinen et al., 2013).

Although IR and Raman spectroscopies are both based on molecular vibrations, it is important to notice that some vibrations are only Raman or IR active. Thus, these techniques give spectra and can be used to complementary each other. For example, symmetric vibrations are always Raman-active but not always IR-active (Ferraro & Nakamoto, 2003; Smith & Dent, 2005). Furthermore, it has been noticed that strong IR absorption occurs for polar molecules whereas Raman scattering is strong for non-polar groupings such as S-S. While the IR bands rise form the change in dipole moment, Raman bands from the change in polarizability of the molecule. (Smith & Dent, 2005) Raman spectroscopy has shown success in the characterization of the secondary structures present in feathers (Barone et al., 2006; Church et al., 2010), and especially disulfide bond could be easily identified in Raman spectra (Barone et al., 2006; Poole et al., 2011; Wojciechowska et al., 1999). Additionally, polarized Raman spectra have been used to observe the protein chain orientation in keratin

fibers (Church et al., 2010; Poole et al., 2011; Rintoul et al., 2000). One example of the possible Raman spectrum for feather keratin is shown in Figure 6.

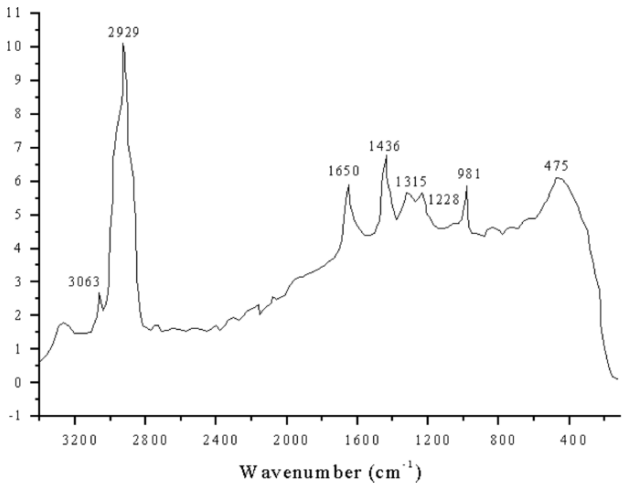

Figure 6. Raman spectrum for feather keratin (Martinez-Hernandez et al., 2005).

Also, NMR spectroscopy can be used to determine the folded structure of the protein as the chemically identical groups within the different environment can be differentiated (Markley et al. 1997). For example, carbonyl group produces a slightly different signal if it is in α-helix or β-sheets (Idris et al., 2013). NMR technique is based on the study of the energy levels of specific atomic nuclei when the sample is placed in a magnetic field. The formed spectra are based on the absorption and emission of electromagnetic radiation of the nuclei. The most common nuclei to study by NMR are ^{13}C and ^{1}H. Usually, in NMR, the samples are dissolved, and NMR is run in liquid-state. However, not all samples are suitable for dissolution. For example, it can be assumed that dissolved feather keratin has different chemical structure compared to the solid form. Then solid-state NMR is an option. In solid, stronger interactions are present, and there is not sufficient motion of the molecules. This means that the measurement takes longer time, and the molecules induce broad peaks. (Markley et al., 1997)

Some NMR studies have been carried out to study the local structure and dynamics in the feather structure (Barone et al., 2005; Barone et al., 2006; Idris et al., 2013). Reddy et al. (2011) used ^{1}H NMR in liquid-state, but only the success of the modification (cyanoethylation) was investigated. In other studies, solid state ^{13}C NMR was used. From these spectra, some of the amino acids can be identified, and interpretations of the secondary structure can be made (Barone et al., 2005; Duer et

al., 2003; Idris et al., 2013). One example of the possible ^{13}C NMR spectrum for feather keratin is shown in Figure 7.

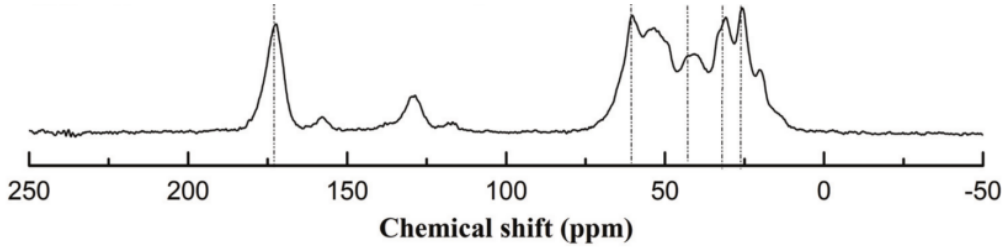

Figure 7. NMR spectrum for feather keratin (Idris et al., 2013).

CD is also an absorption spectroscopy. CD uses circular polarized light, and it is sensitive to the chiralities, conformations, and environments of the molecules. The signal is formed from the interaction between the polarized light and dipoles involved in its absorption and is sensitive to their relative orientations. The resolution of CD is lower compared, for example, to NMR but it gives reasonably accurate results about the fraction of residues that are present in the secondary structure of the protein (Creighton, 2010). Yin et al. (2013) have applied CD in order to study the secondary structure of feather keratin. However, it is important to observe that the samples were characterized in a liquid form and the spectra were obtained in far UV region (180–250 nm). The issue in this technique, considering feather characterization, is that samples are mostly characterized in liquid state, and more specifically as a watery solution. One interesting option for feather characterization could be solid state CD which, at least based on the literature, has not yet been applied for feather keratin.

3.1.5 Crystallinity

The characterization of the crystalline structure in feathers is also very interesting as feathers are considered to be semi crystalline structures (Barone & Schmidt, 2005), and it can be assumed that crystallinity has an important effect on the properties of feather keratin. X-ray diffraction (XRD) crystallography is widely used characterization technique in order to understand the atomic scale structure of the crystallinity of the material sample. This technique is based on diffracted X-ray beams which are focused on the sample. Interaction of X-ray beams with the sample creates secondary diffracted X-ray beams related to the interplanar spacing in the crystalline powder according to a mathematical relation called Bragg's Law. When the diffraction angle and the intensity of the diffracted beams are detected, the specific diffraction pattern

is formed. The diffracted beams not only depend on the atomic arrangement and interplanar spacing but also the atomic species. (Waseda et al., 2011)

In feathers, crystallinity is considered to have an important role in their strength and stiffness (Zhao et al., 2012; Barone & Schmidt, 2005). The study of the crystallinity in feathers has been mainly carried out with XRD (Belarmino et al., 2012; Eslahi et al., 2014; Idris et al., 2013; Khosa et al., 2013; Ma et al., 2016; Pedram Rad et al., 2012; Sun et al., 2009; Tuna et al., 2015; Zhao-Tie et al., 2009; Zhao et al., 2012). XRD has been used to determine the percentage of the crystallinity (Belarmino et al., 2012; Eslahi et al., 2014; Tuna et al., 2015) as well as to differentiate the crystalline structures α-helices and β-sheets from each's others (Eslahi et al., 2014; Idris et al., 2013; Khosa et al., 2013; Ma et al., 2016; Pedram Rad et al., 2012; Sun et al., 2009; Zhao-Tie et al., 2009; Zhao et al., 2012). However, not all authors are consistent with their interpretations which mean that when interpreting the results extra caution must be given. Also, some problems related to the peak overlapping can occur (Idris et al., 2013; Ma et al., 2016; Sun et al., 2009). One example of the possible XRD pattern for feather keratin is shown in Figure 8.

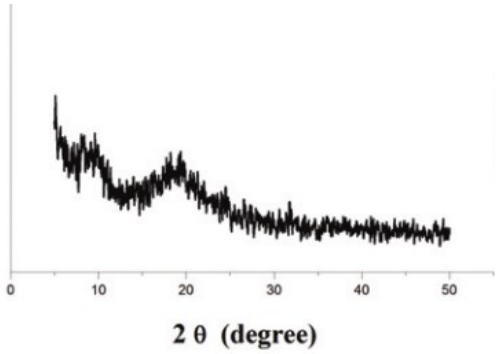

Figure 8. XRD pattern for feather keratin (Idris et al., 2013).

3.1.6 Molecular weight

It has been observed that reasonable determination of the feather keratin molecular weight can be done by reducing all of the S-S bonds followed by solubilization of keratin and measurements of osmotic pressure, turbidity, sedimentation rate and viscosity. Using these techniques, the molecular weight of 10 000 g/mol has been obtained. (Woodin, 1954) The molecular weight of the extracted feather keratin has also been studied by size exclusion chromatography, and more specifically by gel permeation chromatography (GPC) (Ji et al., 2014; Wang & Cao, 2012; Zhao et al.,

2012) and high-performance liquid chromatography (HPLC) (Zhang et al., 2015). SEC is a technique which uses a column in order to sort molecules according to their size in solution. The protein solution (mobile phase) is introduced to flow through the column which is packed with porous material (stationary phase). The mobile phase interacts then with the porous stagnant phase which will lead to the situation in which larger molecules come out and are detected first and the smallest ones last. GPC refers to SEC which is packed with gel (Striegel et al., 2009) while in HPLC, the column is filled with a polar or non-polar material (usually silica or silica supported) which interact with the introduced solution (Ho et al., 2003). As already mentioned, when SEC is carried out the dissolution of keratin is required. This, on the other hand, usually means the destruction of S-S bonds. The obtained results from GPC for feather keratin was quite nicely in respect with the results obtained by Woodin (1954) (Ji et al., 2014; Wang & Cao, 2012; Zhao et al., 2012), and indicated that the extracted keratin was uniform in its molecular weight (Ji et al., 2014; Wang & Cao, 2012). However, it has been observed that using different buffers cause variation in the results (Zhao et al., 2012; Zhang et al., 2015) as well as some degradation of the keratin into amino acids or small polypeptides can occur (Wang & Cao, 2012).

Compared to SEC, matrix-assisted laser desorption/ionization time of flight mass spectrometry (MALDI-TOF MS) is known as a sensitive technique to measure the molecular weight of molecules with high molar masses such as proteins. In this technique, the liquid or solid sample is first mixed with a matrix which performs as energy absorbent. This combination is then focused with a laser beam which causes the ionization and desorption of the molecules within the sample. These ionized molecules are then separated and detected according to their mass-to-charge ratio (m/z). (Hillenkamp et al., 1991) Yin et al. (2013) studied the molecular weight of the extracted feather keratin using MALDI-TOF MS. The used matrix was acid. From the obtained molecular weight, also a number of amino acids in one keratin molecule was interpreted (Yin et al., 2013).

From the techniques described above, MALDI-TOF MS as a simple relatively simple technique is preferred for feather keratin since no dissolution is required. However, as the literature is quite nicely in line when it comes to the molecular weight of feather keratin, the determination of molecular weight comes extremely interesting when different processing methods and their optimization are evaluated.

3.1 Physicochemical properties

Physiochemical properties of feathers play an especially important role when it comes to utilization of feathers in specific material applications. Thus, the techniques to characterize the physiochemical properties are usually applied in studies where some processing, regenerating or modifying have been made. Furthermore, these techniques can be used to complementary the interpretations of the characterization techniques for chemical structure and composition. For instance, microscopy studies can provide important information about the microfibril level structure, and differential scanning calorimetry (DSC) about the crystallinity. Some commonly used techniques to characterize the physiochemical properties of feathers are presented in this section.

3.2.1 Microstructure and morphological features

Microscopies are used to study objects and areas which cannot be seen by the naked eye as they are able to magnify the images from a few times to more than a million times. In feather studies, this means the study of microstructures and morphological features and fine structures of the surface. Microscopic study for feathers has been carried out by using optical microscopy (OM), scanning electron microscopy (SEM) and transmission electron microscopy (TEM). Although these imaging techniques are not able to provide any qualitative or quantitative data, they are excellent techniques to expand the overall understanding.

In OM, the object under study is illuminated by light. The scattered and transmitted light is then collected by a system of lenses to form an image. OM usually enables an imaging with magnification from 2 to 2 000 times. In SEM, the image is formed when focused electron beam is scanned across the specimen. Electrons interact with the atoms on the surface of the specimen, and reflected signals are detected. (Sawyer et al., 2008) The formed signals are able to resolve details with magnification of 20 to 1 $x10^5$ times (Sawyer et al., 2008), and create an image which can be then used, for example, to see the hierarchical structure of the feather, and the surface structure of the keratin fiber (Martinez-Hernandez et al., 2005). Also, TEM is based on the electron beam. In this technique, electron beam is focused through a thin sample. The electrons then interact with the atoms within the sample, and the transmitted electrons are imaged. TEM enables the magnification from 200 to $2x10^6$ times. (Sawyer et al., 2008) Although TEM enables to image the microfibril structure quite nicely (Martinez-Hernandez et al., 2005), the sample preparation is much more complicated compared to OM and SEM (Sawyer et al., 2008).

From these three microscope techniques, SEM is the most applied in feather study. SEM is used to image the raw chicken feathers in order to understand the microstructure and the morphological features of keratin fibers as well as to image the modified, regenerated and applied fibers especially to see the difference compared to the native fibers and their behavior in different applications (Barone & Schmidt, 2005; Belarmino et al., 2012; Fujii & Li, 2008; Giraldo & Moreno-Piraján, 2013; Huda & Yang, 2008; Ji et al., 2014; Ma et al., 2016; Martinez-Hernandez et al., 2005; Pourjavaheri et al., 2016; Reddy & Yang, 2007; Sun et al., 2009; Tuna et al., 2015; Yin et al., 2013; Zhan & Wool, 2011; Zhang et al., 2015; Zhao-Tie et al., 2009). OM has provided imaging of the branched structure of the feathers (Martinez-Hernandez et al., 2005) as well as the imaging of the dispersion of the keratin fibers in the composite material (Pourjavaheri et al., 2016). On the other hand, TEM has shown the capability to show the microfibril and non-crystal structures within the keratin fibers (Fraser & Parry, 2008; Martinez-Hernandez et al., 2005; Wang et al., 2013).

3.2.2 Hydrophilicity and hydrophobicity

As already mentioned, the amino acid content in the feather keratin determines the hydrophilicity and hydrophobicity of the feather keratin. More specifically, it depends on which amino acids are internal or external on the surface. (Schmidt & Jayasundera, 2003) One way to measure the hydrophilicity and hydrophobicity on the feather surfaces is to measure their contact angle. Generally, the contact angle measurement is performed by measuring the tangent (angle) of a liquid drop on the solid surface. The measured angle can be then used to interpret the level of hydrophilicity. (Kwok & Neumann, 1999).The contact angle measurements have been applied for feathers to characterize the surface properties, especially to observe the difference in hydrophobicity between the native feather and regenerated or modified feathers (Sun et al., 2009; Zhao-Tie et al., 2009). In general, it is known that feathers are hydrophobic. Thus, the determination of the hydrophilicity comes especially interesting when feathers are applied in applications where a certain level of hydrophilicity is required.

3.2.3 Thermal stability

The thermal stability of feather keratin has been mainly studied by thermogravimetric analysis (TGA) and differential scanning calorimetry (DSC). Thermal behavior of feather keratin comes especially important when considering the suitability of specific applications and processing methods, such as films and extrusion. As simplified, TGA

measures the mass or the change in mass as a function of temperature or time while DSC determines the quantity of heat that absorbs or releases when sample undergoes a physical or chemical change.

Both, TGA and DSC, are often used in feather studies. In these studies TGA has been mainly used to determine the decomposition of feather keratin structure (Giraldo & Moreno-Piraján, 2013; Hu et al., 2011; Idris et al., 2013; Khosa et al., 2013; Ma et al., 2016; Martinez-Hernandez et al., 2005; Tuna et al., 2015; Ullah & Wu, 2013; Yin et al., 2013; Zhang et al., 2015) while DSC can be used to illustrate the melting or disordering of the crystalline structure as well as the glass transition point in thermoplastically modified feathers (Barone et al., 2006, 2005; Hu et al., 2011; Idris et al., 2013; Khosa et al., 2013; Martinez-Hernandez et al., 2005; Reddy et al., 2011; Schrooyen et al., 2001; Tuna et al., 2015; Ullah & Wu, 2013; Zhang et al., 2015). From both techniques, also the evaporation of moisture can be seen.

4 Feather processing

The unique properties of chicken feathers, such as the high content of keratin, low density, and mechanical durability, combined with their low cost and availability have already shown potential for utilizing them into value added material applications. Some of these material applications could be, for example, electrodes, dielectric materials, biodegradable printed circuit boards, feather composites, films and thermoplastics, absorbents, flame retardants, micro and nanoparticles, and regenerated fibers. However, the poor thermoplasticity, difficulty in dissolving and limited knowledge of processing and products' properties have limited to utilizing of chicken feathers at a larger scale. (Reddy, 2015) Nevertheless, from the environmental and economical point of view, the uniqueness of this raw material makes it an attractive alternative for bioproducts and drives the interest of researchers to study it more. In this chapter, I will discuss more about the processing and regeneration of chicken feathers, and introduce some interesting methods which have been applied for them.

Keratins are known to be insoluble in common polar and non-polar solvents due to extensive disulfide crosslinking, high content of hydrophobic residues and tight packing of α-helices and β-sheets in polypeptide chain which makes feathers challenging to be utilized (Schrooyen et al., 2000; Zhang et al., 2015). Thus, an effective and profitable process to extract and apply feathers is desired (Yin et al., 2013). The desirable solvent for feather dissolution is a solution which enables the

re-crosslinking, does not cause the degradation of the primary protein chains, and is industrially scalable (Poole et al., 2011). Nevertheless, there are three important functional groups in the keratin protein which should be considered when processing, regenerating and modifying feather keratin for material applications. These groups are sulfhydryl group (SH), amino group (NH_2) and carboxylic group (COOH). (Khosa et al., 2013)

For the development of biodegradable materials with good mechanical properties, disulfide bonds between the keratin molecules are preferred (Schrooyen et al., 2000, 2001). Besides the crosslinked disulfide bonds, hydrogen bonding and crystallinity play an important role in the feather strength and stiffness (Zhao et al., 2012; Barone & Schmidt, 2005) which means that also the presence of these interactions in the processed and regenerated feather keratin is desired. This means that after a certain processing method, effective rearrangement should take place. However, to retain the feathers' unique properties after the processing and regenerating has been challenging as the disulfide bonds partly destroy and the amount of secondary and crystalline structures decrease. Some processing methods which have already been applied for bird feathers are extracting the keratin by dissolving in different solvents (Fujii & Li, 2008; Ma et al., 2016; Pedram Rad et al., 2012; Poole et al., 2011; Sharma et al., 2016; J. Wang et al., 2016; Yin et al., 2013) or in ionic liquids (ILs) (Idris et al., 2013; Kammiovirta et al., 2016; Sun et al., 2009; Y. X. Wang & Cao, 2012), grinding and crushing (Barone et al., 2005; Hu et al., 2011; Pourjavaheri et al., 2016), steam flash explosion (Zhang et al., 2015), carbonization and thermal processing (Wang et al., 2013; Zhao et al., 2015), enzymatic hydrolysis (Dalev, 1994; Eslahi et al., 2014), and pyrolysis (Senoz et al., 2013). The chosen processing method is chosen based on the application in which keratin is utilized. Usually, utilization and conversion of feathers require extraction, by dissolving and regenerating, of keratin into suitable biopolymers (Idris et al., 2013). However, in some cases, the mechanical treatment can be enough. For example, if ground feathers are applied as reinforcement in bio-composites (Pourjavaheri et al., 2016).

Next, in this chapter, some methods to convert feather keratin into micro and nanoparticles will be presented. This will then be followed by an introduction to two simple and environmentally friendly processing methods which are steam explosion and extraction of keratin with deep eutectic solvents. These are also the techniques which are applied for feathers in this master's thesis.

4.1 Micro and nanoparticles

One interesting application for feathers is to convert them into keratin micro and nanoparticles. These particles could be then utilized in other applications such as in food, agriculture, cosmetology, medicine and material areas such as in coatings. (Reddy, 2015) Although, as already mentioned, the dissolving of feathers have been challenging due to tight bonding, some attempts have been carried out in order to form nanoparticles from feathers, and some of these techniques will be presented in this section. At the end of this section, also, some techniques to produce keratin powder are presented as in some studies keratin is converted into powder form before further processing. However, these techniques will be discussed only briefly.

Xu et al. (2014) have prepared nanoparticles from chicken feathers to form water-stable nanoparticles for targeted delivery in biomedical applications. In their study, feathers were hydrolyzed using sodium hydroxide (0.1 M) at a ratio of 15:1 with sodium bisulfite for 2 hours at 80℃. The hydrolyzed feather keratin was then precipitated with hydrochloric acid. This keratin precipitation was then washed, dried and pulverized into powder. In order to prepare nanoparticles from this powder, the powder was first dissolved in ethylene glycol at different concentrations. Particles were obtained when water was added to this keratin-ethylene glycol solution followed by ultrasonication. Nanoparticles sized from 50 to 130 nm were obtained. Moreover, the regenerated keratin nanoparticles were investigated to have a smaller amount of tightly packed crystalline structure than raw material. (Xu et al., 2014)

In the study of Fujii & Li (2008), chicken feathers were used to prepare films and particles. In their study, keratin from chicken feathers was first extracted by so-called Shindai method at 50℃ for 24 hours. In this method, ethanol treated chicken feathers were mixed with Tris-HCl (20 mM), thiourea (2.6 M), urea (5 M) and 2-mercaptoethanol (5%) which was then followed by filtration and centrifugation. Protein aggregates were then prepared from this obtained keratin solution by pre-cast, post-cast and soft post-cast method. These protein aggregates were then used to prepare protein particles by mechanical stress using a sonicator. This method was able to convert about 80-90% of the feather into protein solution. (Fujii & Li, 2008) However, no changes in the chemical structure were characterized or reported thus the potential of this method is hard to estimate.

Also, Yin et al. (2013) have used so-called Shindai method to extract the keratin from chicken feathers. Their method included three different steps: ethanol pretreatment,

hydrochloric acid pretreatment, and 2-mercaptoethanol deoxidization. This means that pretreated feathers were immersed in a solution (150 ml) containing urea (0.33 M), sodium dodecyl sulfate (SDS) (0.05 M), 2-mercaptoethanol (0.095 M) and Tris (0.016 M). This mixture was stirred at 70℃ for 2 hours under N_2 atmosphere. The solution was then filtered, acidified and the keratin was precipitated with ethanol in order to obtain the keratin in powder form. This powder was observed to consist of spherical, tightly packed nanoparticles and random arranged porous microstructures. Furthermore, the yield of pure keratin was up to 90%, and the β-sheet conformation was partly destroyed during the extraction process. (Yin et al., 2013)

Pedram Rad et al. (2012) have also made nanoparticles from chicken feathers. Chopped feathers were first dissolved in an aqueous system including urea, ethylene diamine, tetra acetic acid, mercaptoethanol, hydroxyl methyl amino methane and SDS in a N_2 atmosphere at 40℃ for 2 hours. SDS was added to prevent the oxidation of cysteine bonds (the oxidation is observed lead to aggregation of keratin). The dissolution was followed by vacuum filtering and dialysis. In order to prepare keratin sponge, the keratin dispersion was frozen and freeze dried. The actual nanoparticles were prepared by electrospraying which required that the formed keratin sponge was completely dissolved in trifluoroaceticacid (TFA). After electrospraying the formed nanopowder had average particle size of 53 nm and uniform shape. The crystallinity was decreased compared to the raw feather. (Pedram Rad et al., 2012)

Ma et al. (2016) prepared keratin powder before fabrication of keratin membranes and fibers. The extraction of keratin was first carried out by mixing the chicken feathers with solution containing 8 mol/l urea and L-cysteine at 70℃ for 12 hours. The dissolved keratin was then precipitated using hydrochloric acid and sodium sulfate. After washing, the collected precipitate was freeze dried and pulverized with yield of 60%. Before fabrication the membrane and fibers, the keratin had to be once more dissolved in order to carry out the casting process and wet spinning method. The keratin powder, membrane and fiber were then characterized and results were compared with raw chicken feathers. It was observed that the chemical structure (results from FTIR) and thermal stability remained relatively well while the relative crystallinity differed depending on the shaping method. (Ma et al., 2016)

Sun et al. (2009) have also prepared nanoparticles. In their study, ionic liquid (IL) 1-butyl-3-methylimidazolium chloride ([BMIM]Cl) was used to dissolve and regenerate the chicken feathers. The whole feathers were immersed in IL at 100℃ for 48 hours

under an inert atmosphere of N_2.The keratin particles were then regenerated from the solution by adding ethanol or water under vigorous stirring for 30 min. This was followed by filtration of formed particles. In this study, the solubility of feathers was only 23%, and the degree of crystallinity as well as the content of the β-sheets of regenerated feathers were observed to be lower compared to the raw feather. Also, the hydrophobic nature of raw feather changed to hydrophilic in regenerated feathers. (Sun et al., 2009)

In the study of Eslahi et al. (2014), nanoparticles were prepared by enzymatic hydrolysis, followed by ultrasonic treatment. In their study minimum particle size was obtained by using 5 g/l feather and 3.6% enzyme at hydrolysis time of 243 h. In their study it was observed that crystallinity increased and thermal stability enhanced. (Eslahi et al., 2014) However, the time consuming of the process as well as the price of enzymes are high so scaling up this method to industrial scale may not be profitable.

Zhang et al. (2015) processed duck feathers by steam flash explosion (SFE). This step was then followed by grinding and alkali treatment in order to extract the keratin. The recovered keratin was then pulverized. It was observed that the disulfide crosslinks as well as the hydrogen bonds were destroyed from the protein backbone which itself was relatively well retained. Also, the ordered structure was partly lost, and fragmentation of macromolecular chains was found. Moreover, the yield (43%) was relatively low. (Zhang et al., 2015)

Feather fiber powder has also been prepared by mechanical processing. This has been done, for example, in the studies of Barone et al. (2005), Barone et al. (2006) and Hu et al. (2011). In these studies the feathers were ground into powder before further processing. In the study of Barone et al. (2005), the feather fiber powder was obtained by grinding the fibers on a ball mill. This was then followed by modification and film processing (Barone et al., 2005). In the study of Barone et al. (2006), feather fiber powder was prepared as described previously. This powder was then used to prepare blend for extrusion (Barone et al., 2006). Hu et al. (2011) pulverized the chicken feathers using Wiley mill. These powdered feathers were then acetylated and converted into thermoplastic films (Hu et al., 2011). It is important to notice that in milling, the particle size is relatively large and they have no uniform shape (Pedram Rad et al., 2012). Additionally, Wang et al. (2013) prepared chicken feather carbon powder by thermal processing. In their study, feathers were first heated at 210℃ for

26 hours under argon atmosphere. This caused the natural crosslinking of chicken feathers. This step was followed by raising the temperature from 210℃ to 450℃ for one hour which led to formation of final form of the chicken feather carbon powder. In this study, the aim was to prepare supercapacitors from high-capacity carbon prepared from renewable chicken feathers (Wang et al., 2013). Mechanical treatment is also a potential choice to be used as a pretreatment before dissolution. This could ease the solvent accessibility in the feather structure.

4.2 Steam explosion

The current processes to utilize feathers are mainly based on strong acid and alkali hydrolysis, chemical cleavage or other violent reactions. These processes are not eco-friendly and often degrade the feather keratin structure. It has been suggested that efficient biomass converting requires some pretreatment. This could then destroy the structure without degrading it or release the constitutive components, thus improving the solvent accessibility. (Zhao et al., 2012) At the moment, steam explosion is a developing physicochemical pretreatment technique in biomass converting processes. Steam explosion is considered to have advantages like low environmental impact, low capital investment and less use of hazardous process chemicals (Zhang et al., 2014). Also, the high yield, relatively low energy consumption (Tonin et al., 2006) and suitability to larger scale (Zhao et al., 2012) are benefits in this technique. As simplified, steam explosion is based on short time biomass steam cooking at high temperature and pressure followed by explosive decompression. Recently, steam explosion technique is used in some industrial applications for lignocellulosic biomass. However, based on current information, this technique is not used for keratinous biomasses at industrial scale. (Tonin et al., 2006)

Recently, especially, steam flash explosion has gained attention in biomass protein extraction (Zhang et al., 2015). The difference between the conventional stem explosion and steam flash explosion is the time of explosive decompression. In conventional technique the release of high pressure steam requires at least several tens of seconds while in steam flash explosion the decompression is completed in milliseconds (Yu et al., 2012). With the extremely short time the violent treatment under high temperature and pressure for a long time could be avoided and enough force could be achieved to disturb and unfold the dense structure of fibrous proteins (Zhao et al., 2012). It has been suggested that when the decompression time is fast enough, the steam and the water within the biomass expand quickly and escape from the structure resulting the mechanical shearing force to disrupt material's internal

structure (Yu et al. 2012). Nevertheless, steam flash explosion has already shown potential as a pretreatment for feather waste (Zhang et al., 2015; Zhao et al., 2012) or even as processing method for digestible feather meal (Zhang et al., 2014).

4.3 Ionic liquids and deep eutectic solvents

Although the dissolution of keratin is challenging, it can be done even without any pretreatment. Usually, it is done by reduction, oxidation, sulfitolysis or oxidative sulfitolysis of the disulfide bonds present in keratin structure (Poole et al., 2009). However, the chemical which are used to these reactions are often toxic, not environment friendly, poorly recyclable and costly to produce (Idris et al., 2013). Furthermore, also, the need of different reducing agents drives the desire to develop more simple methods (Yin et al., 2013). Currently, ionic liquids (IL) have attracted attention as an environmental friendly and safe alternative to replace traditional organic solvents (Ji et al., 2014). ILs are a group of salts which are in liquid form at relatively low temperatures. This is due to ions' inability to form stable crystal lattice since at least one of the ions has delocalized charge, usually unsymmetrically substituted cation, and one is organic. (Moore, Mangos, Slattery, Raston, & Boulos, 2016) ILs are known as non-volatile, non-flammable, chemical and thermal stable, easily recyclable as well as remarkable soluble (Ji et al., 2014). Moreover, their properties can be relatively easily manipulated by choosing the anions and cations and their ratio carefully according to the need (Wang & Cao, 2012). Feathers have already been successfully dissolved in ILs. Idris et al. (2013) succeeded to dissolve turkey feathers in different kind of ILs with the solubility of 45 %. Sun et al. (2009) dissolved cock feathers in [Bmim]Cl with the solubility of 23 %. Also, Ji et al. (2014) dissolved duck feathers in [Bmim]Cl. However, dissolution was done with help of water and reducing agent, Na_2SO_3. They were able to have solubility of 96.7 % and the yield of extracted keratin was 75.1 %. (Ji et al. 2014) Wang & Cao (2012) dissolved chicken feathers in IL, [HOEMIm][NTf2], in which water and $NaHSO_3$ were applied. They were able to have a yield of 21 % (Wang & Cao, 2012).

Deep eutectic solvents (DES) are today recognized as a class of IL analogues as they share many similar characteristics and properties with ILs. DESs consist of a eutectic mixture of Lewis or Brønsted acids and bases and can contain range of anionic and cationic species. In general, conventional ILs are composed of one type of separate anion and cation. (Smith et al., 2014) Probably the most commonly used and studied DES is choline chloride and urea. In this DES the charge delocalization and this way the premature melting is achieved through hydrogen bonding between the halide

anion and amide moiety. This leads to situation in which the lattice energy and the melting point of the compounds decrease. (Abbott et al., 2004) Commonly, DESs are obtained by the mixture of quaternary ammonium salt with a metal salt or hydrogen bond donor. Like ILs, also DESs are environmental friendly and exhibit low vapor pressure, relatively wide liquid range and non-flammability. However, unlike ILs, DESs are relatively easy and cheap to prepare. (Smith et al., 2014) Additionally, DESs are considered to be non-reactive with water, biodegradable and benign (Abbott et al., 2004).

Today, the use of DESs in the extraction of bioactive compounds has attracted a lot of interest (Zainal-Abidin et al., 2017). DES, choline chloride:urea (mole ratio of 2:1), has already shown potential in keratin extraction. In the study of Moore et al. (2016), wool was successfully deconstructed in top down fabrication process. No yield was reported. It has been suggested that highly polar DES has the capability to attract anions and disrupt the intramolecular forces of the fibrous protein. Also, urea plays an important role in protein dissolution. To begin with, is assumed that electrostatic interactions between urea and polar residues and/or backbones of the proteins can cause the unraveling. Another assumed mechanism suggests the weakening of hydrophobic bonds and loosening of hydrophobic residues which result in easier dissolving. DESs have been suggested to be a gentle extraction medium. (Moore et al., 2016)

5 Scope of the research

The aim of this master's thesis is to validate the selected analytical methods for the native and processed feather characterization and deepen the understanding of the complex structure of the feathers. The chosen methods for the characterization are decided based on the suitability (i.e. the sample should be in solid state when characterization is carried out) and based on the availability of the instruments. A comprehensive characterization for chicken feathers will be done. The goal is to understand the differences in the chemical structures between the different structural parts of the native feathers as well as between the processed and native feathers by using different characterization methods to complementary each other. The focus will be especially on the characterization of the secondary structures. Feathers will be processed by steam explosion and by dissolving feathers in deep eutectic solvent (DES). The chosen DES is selected based on the VTT's patent by Wahlström et al. (2017).

6 Materials and methods

In this section all the materials as well as applied processing and characterization methods are introduced and described.

6.1 Feather feed stock

White waste chicken feathers were supplied by a poultry processing facility of Sada, located in Valencia, Spain. Waste feathers were further washed and sterilized in Toledo, Spain within 24 hours. Before washing, all the unnecessary materials, such as skin and legs, were removed from poultry feathers manually. Feathers were then washed to remove blood, manure and extraneous materials in conventional washing machine (LG Electronics) with hot water in which 300 ml of soap (BETELENE® CLEANER, Betelgeux) was added. Washing was done at 95 ℃ for 2 hours. After washing, feathers were dried in 60 ℃ oven for 24 hours. The drying was then followed by sterilization. Chicken feathers were sterilized in autoclave with pressurized steam treatment at 124 ℃ for 15 minutes.

6.2 Pretreatment of feathers

Most of the analysis requires samples in homogenous form. In order to obtain homogenous samples, feathers were ground by mortar grinder (Fritsch, Germany) through 1 mm and 0.5 mm blades. In order to avoid warming up and burning of the samples and improve the yield of the grinding, the feathers were roughly chopped by scissors and embedded in liquid nitrogen before grinding. The whole feathers were first ground using 1 mm blade. This was then followed by grinding the already ground samples through 0.5 mm blade. In addition to rachises and barbs, the ground whole feather included calamus. The rachis and barbs and barbules were separated tearing them by hand. This way rachises were successfully separated from barbs and barbules. Barbs and barbules were not separated from each other, and they were characterized together. In this work, barbs and barbules together are considered and called as barbs. Both rachises and barbs were ground in the same way as whole feathers, except 0.5 mm blade was not used, and they were ground only through 1 mm blade.

6.3 Steam explosion

The steam explosion was carried out in two batches on 10 l pressurized vessel and for whole feathers. The experiments were performed at 15.5 bar and 203 ℃ for 2 min with the lifting time of 45 s and 1 min 5 s. The lifting time is the time in which the final pressure is reached. The time in which the pressure was released after 2 min residue

time was not possible to be determined in the reactor. However, it is known to be less than a second. The two batches with different lifting times were later combined and characterized together. The steam exploded feathers were further dried in 50 ℃ oven.

6.4 DES fractionation

The extracted keratin was obtained by dissolving and regenerating feather keratin in deep eutectic solvents (DESs). For DES extraction, ground feathers were used (compactor, VTT, Tampere, Finland). The used DES composed of urea (99-100.5%, Sigma-Aldrich, Germany) and sodium acetate (anhydrous powder, extra pure, Honeywell, Germany) in molar ratio 2:1. The eutectic solution was first formed. Urea, sodium acetate and 10 wt% of water (relative to the total mass) were applied to the reactor (Tornado™ Overhead Stirring System, Radleys, UK) at 97 ℃ for 2 h and under 130 rpm stirring. When solution was formed, 4 wt% of ground feathers were applied in the reactor, and the mixture was let to stir for 17 h at 97 ℃ under 110 rpm stirring. Dissolved keratin and DES were then separated from undissolved particles with heated N_2 pressurized (6 bar) filtration. Keratin present in the filtrate was then precipitated and regenerated into water by adding water twice the volume compared to the volume of the filtrate. Water was also used to wash the precipitate. Regenerated keratin was collected from water and DES by vacuum filtration through 90 µm forming fabric, and finally dried at 105 ℃ over night. The separation chart of DES fractionation is presented in Figure 9.

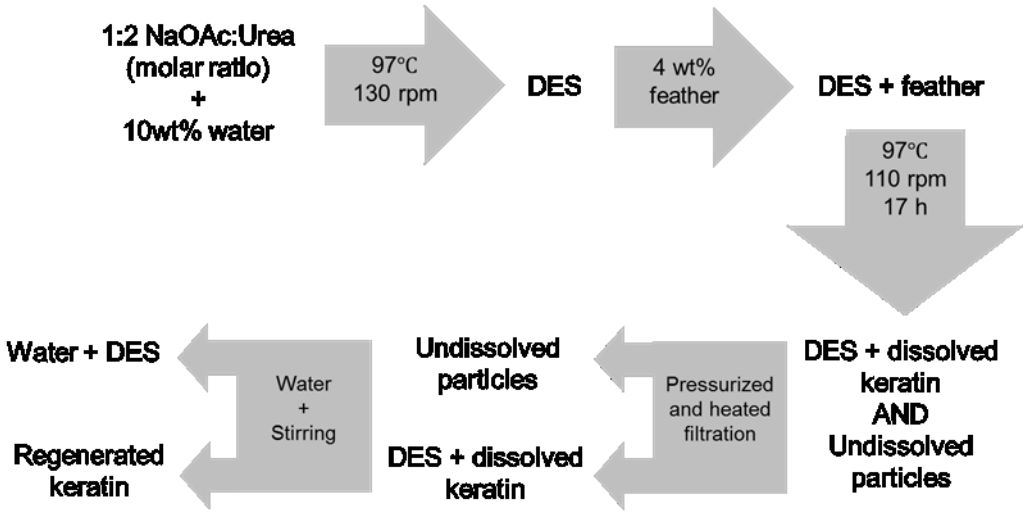

Figure 9. The separation chart of the DES fractionation.

6.5 Optical microscopy

Microscopy studies were carried out by using optical microscopies; stereomicroscopy and brightfield and fluorescence microscopy. Imaging were done for raw and processed chicken feathers.

6.5.1 Stereomicroscopy

Overall appearance of the samples were examined with Zeiss SteREO Discovery.V8 stereomicroscope equipped with Achromat S 0.5x objective (Carl Zeiss MicroImaging GmbH, Göttingen, Germany) and imaged using an Olympus DP-25 single chip colour CCD camera (Olympus Life Science Europa GmbH, Hamburg, Germany) and the Cell^P imaging software (Olympus).

6.5.2 Brightfield and fluorescence microscopy of embedded feather samples

Feather samples were embedded in hydroxyethyl methylacrylate resin (Leica Historesin embedding kit, Leica Microsystems, Heidelberg, Germany) by keeping them first submerged in liquid resin for 7 days in room temperature and then polymerizing the resin as recommended by the manufacturer. Polymerized samples were sectioned (2 µm sections) in a rotary microtome HM 355S (Microm Laborgeräte GmbH, Walldorf, Germany) using a tungsten carbide knife. The sections were transferred onto glass slides and stained. Protein in the sections was stained with a 0.2% (w/v) Ponceau S (P-3504 / (6226-79-5 CAS), Sigma, St. Louis, MO, USA) in 3% trichloroacetic acid overnight followed by rinsing. Protein stained with Ponceau S appears red when imaged in brightfield. For structural visualisation, the sections were stained with 0.5% Oil Red O (BDH Chemicals, Poole, Dorset, UK) in 70% ethanol for 2 min followed by rinsing with water, and drying. In exciting light (epifluorescence, 450-490 nm; fluorescence, >515 nm), the microstructure of the samples appears mainly in various shades of green. Oil Red O is normally used as a lipid stain showing fat containing structures in orange. The stained samples were examined with a Zeiss AxioImager M.2 microscope (Carl Zeiss GmbH, Göttingen, Germany). Micrographs were obtained using a Zeiss Axiocam 506 CCD colour camera (Zeiss) and the Zen imaging software (Zeiss).

6.6 Elemental analysis

Elemental analysis (C, H, N, S and O) was performed using FLASH 2000 series analyzer. Elemental analysis were carried out for ground whole feathers, rachises and barbs as well as for steam exploded feathers and DES extracted keratin. Before analysis, samples were dried in 105℃ oven over night in order to remove excess

moisture. Average value of two parallel samples were measured and reported. The protein content was further calculated according to Kjeldahl method described in the book of Godfrey & Reichelt (1982).

6.7 Amino acid analysis

Amino acid content was analyzed for ground whole feathers, rachises and barbs as well as for steam exploded feathers and regenerated keratin. Samples were first oxidized in order to stabilize methionine and cysteine. This was done by adding oxidation solution which consists of 45 ml of formic acid-phenol solution (89 wt% of formic acid (Sigma-Aldrich), 11wt% of H_2O ELGA, 0.5wt% of phenol (Sigma-Aldrich)) and 5 ml of hydrogen peroxide (Sigma) for 16 h at 0°C. The following step was acid hydrolysis which was done in order to disperse the polypeptide chains in their amino acids and release them into solution. The samples were hydrolyzed with HCl (6N, Alfa Aesar) at 110 °C for 24 h. This was then followed by derivatization of free amino acids with 6-aminoquinoyl-N-hydroxysuccinimidyl carbamate, 6-aminoquinoline-N-succinimidyl-ester (Synchem UG & Co. KG Germany). Finally, derivatized samples, standards and blanks were analyzed with ultra-performance liquid chromatography (UPLC; Acquity Ultra Performance LC; Waters, Milford, MA, USA). The quantitative amino acid composition was determined by calibration with Amino Acid Standard (Sigma-Aldrich, USA) as external standards and L-Norvalin (NVA) as internal standard. For each samples three parallel samples were done, and average was reported.

6.8 ATR-FTIR

The chemical composition of the ground native and processed chicken feathers were characterized with an FTIR spectrometer equipped with an ATR diamond crystal (Thermo Scientific Nicolet iS50, USA). All spectra were acquired in transmission mode with 32 scans with a spectral range of 4000–400 cm^{-1} and spectral resolution of 4 cm^{-1}. Several spectra were collected from different locations of each samples, and the average of these spectra were used in the analysis. The spectra were processed with OriginPro 2017 software. Deconvolution of the bands was carried out using OriginPro 2017 software (Multiple Peak Fit) and Gaussian functions. Deconvolution was done based on the studies of Tsuboi et al. (1991) and Rintoul et al. (2000).

6.9 Visible light Raman

Raman spectra of rachis and barbs sections (preparation described in 7.2.2 p. 24) were collected using a Witec Alpha300 microspectroscope (Witec GmbH, Ulm, Germany) equipped with a 532 nm laser and grating 600 g/mm. The spectra were collected through a 100x air objective (Nikon, NA: 0.90) and the collection time was 30-50 s for a single spectrum. The laser beam was focused on a micrometer sized spot on the samples. Molecular orientation within the sample was determined by measuring the anisotropic response of the sample to different polarized incident radiation (532 nm). This was done according to the study of Galvis et al. (2016). The polarization angle of the laser was rotated using a half-wave plate in the optical pathway. The spectra were obtained with polarizations of 0°, 30°, 60° and 90° of the incident radiation. The spectra were detected using a CCD camera (Andor Newton DU970-BV, Andor Technology plc, Belfast, UK). Raman images were collected using the same spectroscope as above but using 20x and 100x air objectives. This imaging enabled the accurate spot for the measurement. The data was processed with WITec Project 2.10 and OriginPro 2017 software. Deconvolution of the bands was carried out using OriginPro 2017 software (Multiple Peak Fit) and Gaussian functions. Deconvolution was done based on the studies of Schmidt and Jayasundera (2003) and Rintoul et al. (2000).

6.10 XRD

X-ray powder diffraction (XRD) was used to determine the semi crystallinity of all five ground feather samples. A Philips diffractometer (model PW 1130/00) was used with Ni-filtered Cu Kα radiation (λ = 1.541 Å). The data was obtained with geometry in which the sample was kept in place and tube and counter was in motion. X-ray beam was generated at 45 kV and 30 mA. Diffraction intensities were recorded with 2θ ranging from 4° to 60° at a step size of 0.079° and scan step time of 390 s. The data was processed using X'Pert and OriginPro 2017 software. Deconvolution of the peaks was carried out using OriginPro 2017 software (Multiple Peak Fit) and Lorentz functions. Deconvolution was done based on the study of Cao & Billows (1999).

6.11 Solid-state NMR

The ^{13}C cross polarization (CP) magic angle spinning (MAS) NMR measurements were performed using an Agilent DD2 600 NMR spectrometer with magnetic flux density of 14.1 T, and equipped with a 3.2 mm T3 MAS NMR probe operating in a double resonance mode. Samples were packed in ZrO_2 rotors, and MAS rate in experiments was 10 kHz. A total of 10,000 scans were accumulated using a 1.3 ms

contact time and a 6.0 s delay between successive scans. In all experiments protons were decoupled using SPINAL-64 proton decoupling with a field strength of 80 kHz. 90 degree pulse durations and Hartmann-Hahn match for cross polarization were calibrated using α-glycine. The chemical shifts were externally referenced via adamantane by setting the low field signal to 38.48 ppm. The spectra were processed using TopSpin 3.5 and OriginPro 2017 software. Deconvolution of the peak was carried out using OriginPro 2017 software (Multiple Peak Fit) and Gaussian functions. Deconvolution was done based on the studies of Duer et al. (2003), Nishikawa et al. (1998) and Idris et al. (2013).

7 Results and discussion

7.1 Pretreatment and processing of feathers

In separation process, in which rachises and barbs and barbules were separated in order to determine their structural differences, it is important to notice that when barbs and barbules were teared from the rachis, some strips of the rachis outer layer left attached to the barbs. This on the other hand, may have an effect to the characterization as the ratio between the outer layer and inner structure is slightly distorted. In separation process, it was measured that the rachis covers approximately 44 % of the weight of the feathers under investigation while barbs and barbules cover the remaining portion. Before the separation, calamus was cut off. Moreover, in order to obtain as homogenous material as possible for the characterization methods, whole feathers, rachises and barbs were ground. There were no major differences in the grinding process.

The feathers were further processed in order to optimize the best characterization methods to identify the changes taking place in the chemical structure during the processing. The feathers were first stem exploded. The yield in steam explosion was 98 %, respectively. The small mass loss is due to the sticking of the material in the container. The end product was heterogeneous, lightly brown granular like material which was relatively easily converted as homogenous powder like material by mechanical treatment. The transfer of color from white to light brown indicate that changes such as degradation in the chemical structure have occurred. The steam explosion was done in two batches which differed from each other only by the time in which the final pressure was reached. It was noticed that with the lower lifting time (45 s) feathers burned onto reactor surface, and the end product was harder

compared to the steam explosion with higher lifting time (65 s). Before drying, the product from first batch was rubbery like, and difficult to clean from the reactor.

Besides the steam explosion, also, DES fractionation for the ground feathers was carried out. The yield of DES extracted keratin was 64.7 % in respect to the filtrate which came through the pressurized filter system. Not all DES, which included the dissolved and undissolved feathers, was able to be filtrated due to high viscosity and solidification of the DES as the filter cooled down. This is why, it is suggested, that, at least in the lab scale, the feather portion should be less than 4 wt% or the filtration system should include continuous heating. It is important that DES do not solidify before filtering. Furthermore, keratin in the filtrate was easily precipitated in water as the most of the regenerated keratin was insoluble and DES soluble in water. After vacuum filtration, the obtained keratin precipitate was light brown in color and had fluffy structure while after drying it had hard and fragile granular like structure with dark brown color. This material was then easily converted into sandy like material with small particle size by mortar. The dark brown color of the regenerated keratin indicates that the chemical structure has been changed.

7.2 Optical microscopy

Stereomicroscopy was used to show the overall appearance of the branched feather structure (Figure 10a). Also, the structural differences in the ground rachis can be visualized with the stereomicroscopy. The inner structure appears as foamy and powdery solid structure while the outer layer is clearly tighter fibre like structure (Figure 10b). It is assumed that the inner structure is light honeycomb structure which is surrounded by protective outer layer. In the ground barbs, it is not possible to clearly distinguish different structures (Figure 10c). Some foamy and powdery like structure can be identified (see the arrow in Figure 10c). However, it seems that the barbs consist mostly from the fibre like structure which are assumed to be outer layer. This was expected as the barbs are smaller in size than rachis (Figure 10a) which means that their surface area is larger. It can also be seen that in the ground barbs there is more external fibrillation (Figure 10c) compared to the ground rachis (Figure 10b) although they were ground in the same way and under the same conditions. This could indicate that the structure of the rachis is more resistant to mechanical grinding.

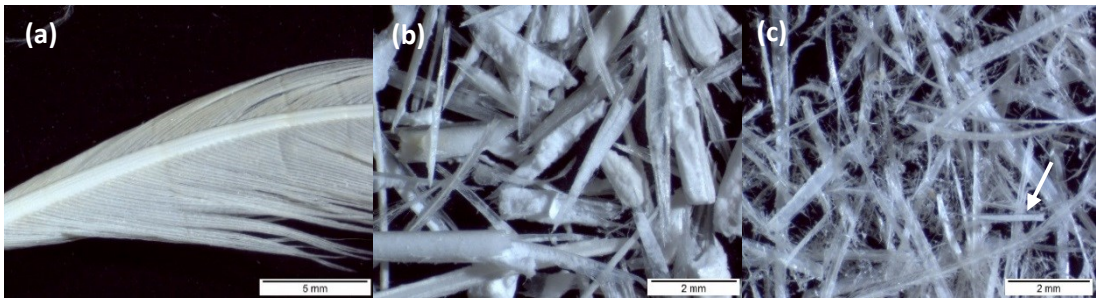

Figure 10. Overall appearance of the feather (a), ground rachis (b), and ground barbs (c).

Feathers were embedded in resin which was further polymerized and sectioned. This was done in order to visualize the longitudinal and cross sections of the feathers. The sectioned samples were further stained with Ponceau S and Oil Red O in order to identify the microstructural differences (Figure 11). Figure 11a represents rachis which is diagonally cut and stained with Ponceau S. Ponceau S is a protein dye which appears as red. In general, it can be assumed that stronger color indicates for higher amount of protein. From Figure 11a, the inner honeycomb structure and outer layer can be easily identified. The outer layer is assumed to be fibrous structure. The diagonal cut allows larger area of the outer layer to be exposed. The uneven coloring in the outer layer such as the darker color on the edges and the darker dots in the diagonal section indicate various protein structures.

The structural differences of the rachis can also be seen in cross sectional Oil Red O stained cut (Figure 11) and in longitudinal Ponceau S stained cut (Figure 11c). Oil Red O is usually used to visualize lipid structures as orange. However, in these feather studies, the washing of the feathers has probably removed most of the fat, and the exciting light of the fluorescence microscopy causes the microstructures appear in different shades of green. Again, different shades indicates different structures. It is also notable that with the fluorescence microscopy all the structures are visible not only proteins. In Figure 11b, oval structures can be seen in the outer layer of rachis. These structures appear either as bright green or as darker green on smooth green background. These oval structures could indicate for the fibrous structure. As already mentioned, feathers are considered as keratin fiber reinforced composites which consist of crystalline axially oriented filaments embedded in an amorphous, non-fibrous matrix (Feughelman, 2002; Filshie, 1962; Martinez-Hernandez et al., 2005; McKittrick et al., 2012). In Figure 11c, the protein dye seem

to be adhered oriented with different shades of red. These shades indicate different protein structures present in the rachis while the oriented color adhesion could indicate for the axially oriented fibrous structure. However, the interpretations of the fibrous structure based on the microscopy images and staining have to be treated with caution. The keratin orientation will be discussed more in Raman studies.

Figure 11d illustrates the longitudinal cut and Ponceau S stained barb. Again, the inner honeycomb structure and fibrous outer layer can be identified. When barb is compared to rachis (Figure 10c) in which barbs are attached, a size difference can be seen. The sizes of the rachises and barbs vary a lot depending on the size of the feather. However, it is suggested that the size difference is considerable. The outer layer of barb is much thinner than the outer layer of the rachis which has an effect, for example, in the processing as was seen in Figure 10a&b.

In Figure 11e, Ponceau S stained barbules are presented. Barbules are the tertiary structures in the feather, and they are attached to barb. When barbules and barb (Figure 11d&e) is compared, it can be seen that the size difference is smaller than what it was between rachis and barb. Moreover, no honeycomb structure can be recognized but rather nodes which are evenly distributed along the barbules. These nodes are considered to be junction points in which one segment penetrates through the cross section of another segment (Senoz et al., 2013). It has been suggested that they are related with memory properties and are similar to the scales present in wool (Martinez-Hernandez et al., 2005). The nodes in the barbules stain more strongly (Figure 11e) which could indicate to high amount of protein structures. It could suggest that these points are structural growth points and the protein is not yet organized there. Additionally, the nodes have shown to be vulnerable points for fracture due to low cross sectional area in which stress reaches a local maximum (Senoz et al., 2013).

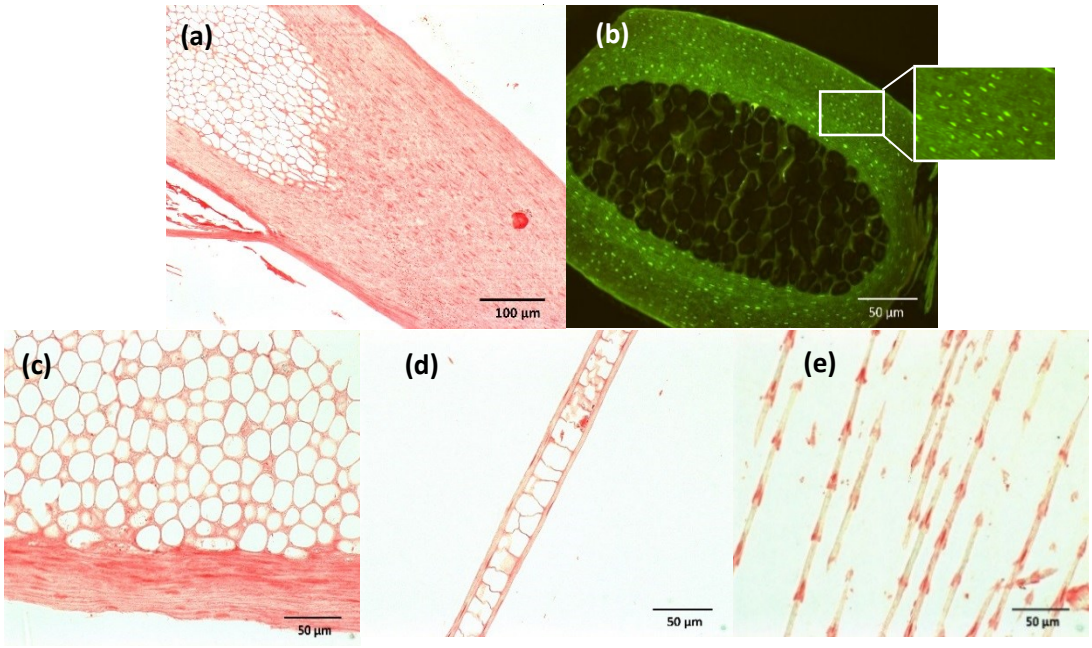

Figure 11. Brightfield imaged, diagonally cut and Ponceau S stained rachis (a), autofluorescence image of cross sectioned rachis (b), as well as Brightfield imaged longitudinal cut and Ponceau S stained rachis (c), barb (d) and barbules (e).

Figure 12 illustrates the steam exploded feathers and DES extracted keratin. After steam explosion the color of the feathers changes from white to light brown which indicates to changes in chemical structures (Figure 12a). Also, different structures can be detected from the overall appearance which means that the steam explosion was not able to form homogenous keratin material and different feather structures respond differently to it. In the cross sectioned and stained steam exploded feather samples (Figure 12b&c), the destruction of clear feather structures can be seen, and the structure is rather matrix than ordered hierarchical structure. Also, some shade differences as well as residues from the original structure can be seen. This supports the earlier conclusion that the steam explosion was not able to form homogenous product. Like after steam explosion, also the color of regenerated keratin is brown (Figure 12d) which is attributed to changes in the chemical structure. The color of regenerated keratin is darker than the color of steam exploded feather which is probably due to higher drying temperature. The cross sectioned samples of regenerated keratin (Figure 12e&f) indicate that the keratin regenerates and recrystallizes as uniform matrix with some structural differences.

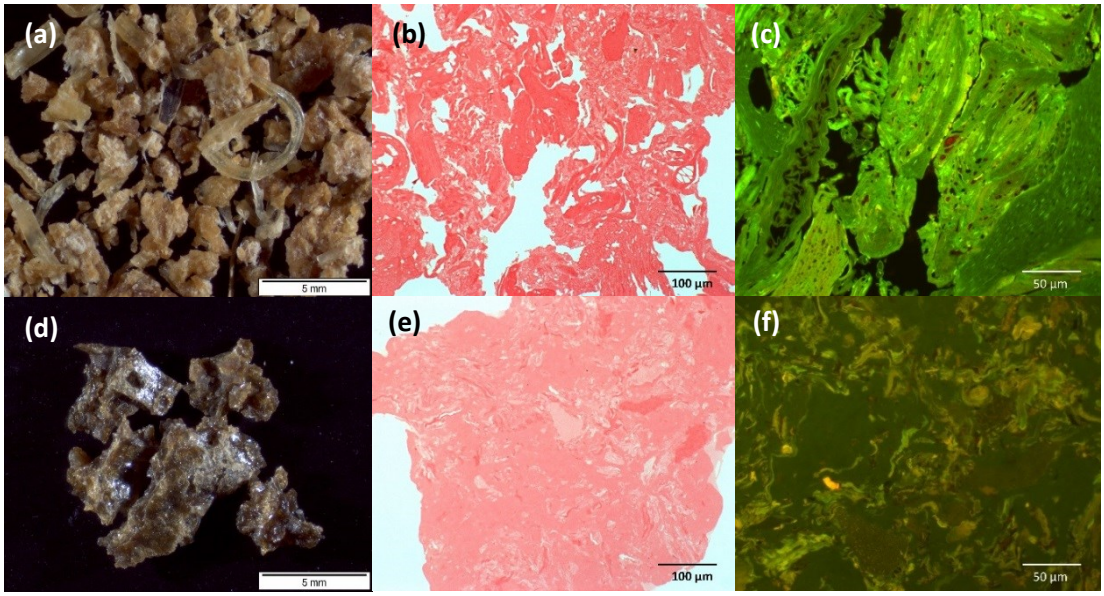

Figure 12. Steam exploded feathers (a,b,c) and DES extracted keratin (d,e,f): overall appearance (a,d), Brightfield imaged, cross sectioned and Ponceau S stained samples (b,e), and autofluorescence image of cross sectioned and Oil Red O stained samples (c,f).

7.3 Elemental analysis

The elemental content was determined in order to deepen the understanding of the chemical composition of the feathers under investigation. The results (table 1) are similar with the ones found in the literature (Aguayo-Villarreal et al., 2011; Tuna et al., 2015; Zhao-Tie et al., 2009), and indicate that, in the ground feathers, carbon (C) is the most abundant element. Furthermore, the content of oxygen (O), nitrogen (N) and hydrogen (H) is higher than the content of sulphur (S). However, in protein chemistry, from these elements, S is considered as one of the most interesting ones as it plays an important role in the properties and reactions of proteins (Benesch, 2012). In feather keratin, S is present in cystine disulfide bonds (S-S), in cysteine free thiol groups (SH) or in methionine. Because the content of methionine is low (Table 3) and it is assumed that the amount of free thiol groups is less than 5 %, almost all the sulphur is considered to locate in disulfide bonds. (Schrooyen et al., 2000) From the table 1, it can be seen that there is no considerable differences in the sulphur content between the native feather and its parts. However, when the whole feather is compared to steam exploded feather and regenerated keratin, the sulphur content decreases clearly. This may indicate that the cystine have cleaved and the free thiol groups have then further reacted. Nevertheless, the cleavage of one disulfide bridge yields two cysteine residues and their free thiol groups. These thiol groups are then

likely to further react, for example, to sulfoxyl compounds or formed sulphur containing volatiles. (Zhang et al., 2014) Nevertheless, it can be assumed that the disulfide crosslinking between cysteine residues is at least partly destroyed. This has then an effect to the protein folding and to the association with the other polypeptide chains (Alberts et al., 1994). In feather studies, elemental analysis is especially suitable to characterize the differences occurring in S content after some specific treatment. In order to understand the function and correlation of other elements to the material properties, extensive research which combines other techniques is required.

Besides the sulphur content, the content of nitrogen can be informative as the most of the indirect protein determinations are based on the nitrogen content. One of these determinations is Kjeldahl method. In samples which include also other substances than protein (in feathers there are, for example, fat and water), the total protein content is determined by multiplying the nitrogen content by a factor which corresponds to an average nitrogen content. In feathers, this factor has been suggested to be 6.66 as the protein nitrogen content in feathers has been determined to be 15 %, respectively. (Godfrey & Reichelt, 1982) This method was also applied for the studied feathers and the results can be seen in Table 2. First of all, the calculated protein contents are only directional and are based on the factor given in literature. The exact results would require a factor corresponding to the nitrogen content of the individual protein (Godfrey & Reichelt, 1982). Secondly, it has to be noted that the use of protein nitrogen content in regenerated keratin is not valid as the residuals of DES can increase the nitrogen content very easily. However, based on the results obtained (Table 2), it is suggested that the rachis contains most protein, and in processing no major differences in the protein content are observed when compared to the whole feather.

Table 1. The elemental composition of raw and processed chicken feathers.

Sample	Component (%)				
	Nitrogen	Carbon	Hydrogen	Sulphur	Oxygen
Whole feather	15.13 ± 0.50	52.73 ± 0.21	7.20 ± 0.08	2.09 ± 0.02	24.85 ± 0.18
Rachis	16.50 ± 0.24	50.94 ± 0.16	6.94 ± 0.01	2.20 ± 0.00	25.88 ± 0.37
Barbs	14.74 ± 0.03	52.20 ± 0.32	7.22 ± 0.11	2.17 ± 0.01	25.71 ± 0.18
Stem exploded	15.37 ± 0.41	53.51 ± 0.18	7.43 ± 0.00	1.76 ± 0.05	24.93 ± 0.21
Regenerated keratin	14.84 ± 0.13	52.62 ± 0.11	7.56 ± 0.01	1.24 ± 0.01	20.70 ± 0.10

Table 2. The protein content of the native and processed feathers calculated by using the Kjeldahl method.

Sample	Protein content (%)
Whole feather	101
Rachis	110
Barbs	98
Stem exploded	102
Regenerated keratin	99

7.4 Amino acid analysis

Amino acid analysis was carried out in order to deepen the understanding of the chemical composition and structure of the feather samples. Table 3 gives the amino acid contents for all ground feather samples. The results are reported in actual amount (mg/g) as well as in proportional percentage (% Total AA). Before analyzing the results, the destruction of some amino acids should be taken into account. In the literature, it is stated that the feather structure is about 90 % of protein (Fraser et al., 1972) which means that the amount of all detected amino acids should be approximately 900 mg/g. However, from the sum, it can be seen that only 650-740 mg/g of the amino acids were detected. This means that quite remarkable destruction of amino acids has taken place. The highest amount and the lowest standard deviation of detected amino acids were found to be in the rachis. This could suggest that the rachis tolerated best the acid hydrolysis. However, it has to be taken into account that the rachis was also observed to have the highest content of protein (Table 2).

From the feather samples, 17 different amino acids can be detected (Table 3). The most abundant amino acids are found to be Ser, Glu, Pro, Cys, Val and Leu, respectively, while the content of His, Lys, Tyr and Met is the lowest. In the study of Yin et al. (2013), it was observed that during the amino acid analysis, the content of Asn, Gln, Cys, Ser, Thr and Trp in the feather samples were inaccurate due to breakages during the acid hydrolysis. It has to be also noted that the amino acid composition in different feathers varies, for example, due to breed, feed and environment (Martinez-Hernandez et al., 2005).

It has been stated that the amino acid composition determines the shape of the protein (Alberts et al. 1994) which is why it has also been used to predict the secondary structure of the protein (Chou & Fasman, 1974). Additionally the shape of the fibrous proteins is considered to be dominated by the secondary structure (Voet

& Voet, 2004). Table 4 presents the nature of different side groups of the amino acids which are most present in feather structure and their tendency to promote or break the ordered secondary structures. The tendency is used to predict the protein conformation. However, the prediction is derived for globular proteins, not for fibrous proteins in which many repetitive amino acid sequences are present. This means the prediction should not be indiscriminately applied for feather keratin. (Chou & Fasman, 1974) From Tables 3 and 4, it can be seen that the most of the amino acids present in feather keratin are hydrophobic. In literature it has been stated that the hydrophobic forces and interactions are thermodynamically important in driving the protein folding. In general, it has been suggested that amino acids with conformational flexibility have tendency to cover and protect the hydrogen bonding of the protein's backbone are more likely to form α-helix while amino acids with bulky side chains tends to form β-sheets. Breakers, on the other hand, may form too weak hydrogen bonds or have electrostatic interactions with the backbone atoms. (Neil & DeGrado, 1990) In addition, it has been observed that the amino acid distribution in feather keratin is un-uniform. The central of the polypeptide chain is considered to be rich in hydrophobic residues and β-sheet while terminal regions are concentrated in cysteine residues and are almost missing the ordered secondary structure. (Arai et al., 1983) The three most abundant amino acids in all studied feather samples are Ser, Glu and Pro. These all three amino acid types are considered as breakers in β-sheet while Pro is also considered as a breaker in α-helix and Glu as a promoter in α-helix (Chou & Fasman, 1978).

Considering the different structural parts of the native feathers, the largest differences are between the rachis, and the whole feather and barbs (Table 4). From the proportional percentage, it can be seen that the percentage of Arg, Glu, Thr, Cys and Ile the in rachis is less than in whole feather and barbs. However, when the actual content of these amino acids is compared, no major differences are observed. The only exception is Ile whose actual content in rachis is less than in whole feather and barbs. Ile is considered as hydrophobic amino acid which has promoting effect in β-sheets (Chou & Fasman, 1978; Martinez-Hernandez et al., 2005). Probably, the more noticeable differences in both, in the proportional percentage as well as in the actual content, can be observed in the content of Gly, Ala and Leu. The content of these amino acids is higher in the rachis than in the whole feather or in the barbs. From these amino acids Ala and Leu are hydrophobic and considered to promote α-helix while Gly has conformational specialty and is considered to break the α-helix structure

(Chou & Fasman, 1978; Martinez-Hernandez et al., 2005). However, as already mentioned, the prediction of the secondary structure based on the amino acids, is not derived for fibrous proteins, and it only gives proposals. The amino acid content and the predictions made based on them can be used to support the results obtained from other techniques.

Between the native feather and processed feathers, the largest difference is in the Cys content which supports also the results from elemental analysis as the content of Sulphur decreased. The content of Cys residues decrease significantly in both, in actual amount as well as in proportional percentage. Additionally, the decrease is greater in regenerated keratin than in steam exploded feathers. The results indicate the destruction of cystine and Cys upon processing. Also, small decrease in the actual content of Ser can be observed after steam explosion and DES extraction. Ser is a hydrophilic amino and considered as a breaker in β-sheets (Chou & Fasman, 1978; Martinez-Hernandez et al., 2005). Besides the differences in Cys and Ser, no major changes are observed.

Due to extensive processing protocol and inaccuracy (the destruction of some amino acids and standard deviation) of the acid hydrolysis in amino acid analysis, it is not suggested to be applied for characterization of processed feathers which are utilized in material applications. For these kind of applications other properties such mechanical and thermal properties, are more interesting ones. However, amino acid analysis can provide information to support result from other methods. It also plays an important role, for example, when feather are used for feed purposes and nutrient rich materials are desirable (Saarela et al., 2016).

Table 3. The amino acid content of native and processed chicken feathers presented as actual amounts (mg/g) and as proportional percentages (% Total AA).

Amino acid	Whole feather	Rachis	Barbs	Steam exploded	Regenerated keratin
	mg/g	mg/g	mg/g	mg/g	mg/g
Histidine (His)	3.4 ± 0.1	2.1 ± 0.3	2.4 ± 0.1	3.7 ± 0.5	4.8 ± 0.0
Serine (Ser)	**86.5 ± 1.6**	**91.3 ± 1.2**	**83.2 ± 2.0**	**81.6 ± 4.4**	**75.3 ± 3.5**
Arginine (Arg)	**44.7 ± 2.1**	**42.8 ± 1.1**	**41.6 ± 1.0**	**44.0 ± 4.2**	**49.9 ± 2.3**
Glycine (Gly)	**45.5 ± 1.8**	**61.1 ± 0.7**	**43.4 ± 0.1**	**47.1 ± 2.8**	**48.1 ± 2.5**
Aspartic acid (Asp)	**41.8 ± 2.4**	**47.9 ± 0.2**	**40.6 ± 0.5**	**40.7 ± 3.6**	**43.9 ± 2.1**
Glutamic acid (Glu)	**70.5 ± 1.2**	**71.1 ± 0.5**	**67.3 ± 1.8**	**71.2 ± 6.3**	**72.7 ± 4.4**
Threonine (Thr)	**31.4 ± 1.8**	**29.8 ± 0.7**	**30.9 ± 0.4**	**29.0 ± 2.4**	**32.9 ± 1.6**
Alanine (Ala)	**25.6 ± 1.0**	**43.0 ± 1.6**	**23.4 ± 0.3**	**27.2 ± 1.8**	**28.2 ± 1.3**
Proline (Pro)	**69.1 ± 3.8**	**71.5 ± 0.3**	**67.7 ± 1.3**	**65.8 ± 4.7**	**70.6 ± 3.9**
Cysteine (Cys)	**59.8 ± 1.2**	**60.9 ± 1.5**	**61.3 ± 0.6**	**34.7 ± 2.9**	**18.7 ± 0.8**
Lysine (Lys)	8.1 ± 1.5	4.4 ± 0.4	6.0 ± 0.4	8.9 ± 2.3	5.3 ± 0.1
Tyrosine (Tyr)	16.2 ± 0.5	12.0 ± 0.5	14.8 ± 0.3	16.3 ± 1.3	15.6 ± 0.9
Methionine (Met)	3.9 ± 0.1	2.7 ± 0.2	3.2 ± 0.1	4.4 ± 0.6	5.0 ± 0.2
Valine (Val)	**49.4 ± 2.7**	**56.9 ± 1.4**	**49.1 ± 1.2**	**49 ± 4.5**	**53.1 ± 3.3**
Isoleucine (Ile)	**32.0 ± 1.8**	**28.1 ± 0.5**	**30.6 ± 0.4**	**31.2 ± 3.1**	**37.5 ± 2.0**
Leucine (Leu)	**57.2 ± 2.4**	**74.0 ± 0.6**	**53.1 ± 0.7**	**56.7 ± 4.2**	**57.7 ± 2.8**
Phenylalanine (Phe)	**35.9 ± 0.5**	**41.0 ± 1.6**	**34.3 ± 0.1**	**34.8 ± 2.8**	**38.2 ± 1.7**
SUM	**680.8 ± 24.6**	**740.6 ± 6.0**	**652.9 ± 8.7**	**646.2 ± 50.7**	**657.5 ± 31.6**

Amino acid	% Total AA	% Total AA	% Total AA	% Total AA	% Total AA
His	0.5	0.3	0.4	0.6	0.7
Ser	**12.7**	**12.3**	**12.7**	**12.6**	**11.5**
Arg	**6.6**	**5.8**	**6.4**	**6.8**	**7.6**
Gly	**6.7**	**8.2**	**6.7**	**7.3**	**7.3**
Asp	**6.1**	**6.5**	**6.2**	**6.3**	**6.7**
Glu	**10.4**	**9.6**	**10.3**	**11.0**	**11.1**
Thr	**4.6**	**4.0**	**4.7**	**4.5**	**5.0**
Ala	**3.8**	**5.8**	**3.6**	**4.2**	**4.3**
Pro	**10.1**	**9.7**	**10.4**	**10.2**	**10.7**
Cys	**8.8**	**8.2**	**9.4**	**5.4**	**2.8**
Lys	1.2	0.6	0.9	1.4	0.8
Tyr	2.4	1.6	2.3	2.5	2.4
Met	0.6	0.4	0.5	0.7	0.8
Val	**7.3**	**7.7**	**7.5**	**7.6**	**8.1**
Ile	**4.7**	**3.8**	**4.7**	**4.8**	**5.7**
Leu	**8.4**	**10.0**	**8.1**	**8.8**	**8.8**
Phe	**5.3**	**5.5**	**5.3**	**5.4**	**5.8**
SUM	**100**	**100**	**100**	**100**	**100**

Table 4. The nature of the functional groups present in amino acids (Martinez-Hernandez et al., 2005)*, and the tendency of amino acids in the secondary structures* (Chou & Fasman, 1978)*.*

Amino acid	Nature of side chains	α-helix	β-sheet
Ser	Hydrophilic	Neutral	Breaking
Arg	Positively charged	Neutral	Neutral
Gly	Conformationally special	Breaking	Neutral
Asp	Negatively charged	Neutral	Neutral
Glu	Negatively charged	Promoting	Breaking
Thr	Hydrophilic	Neutral	Promoting
Ala	Hydrophobic	Promoting	Neutral
Pro	Conformationally special	Breaking	Breaking
Cys	Hydrophobic	Neutral	Promoting
Val	Hydrophobic	Promoting	Promoting
Ile	Hydrophobic	Neutral	Promoting
Leu	Hydrophobic	Promoting	Promoting
Phe	Hydrophobic	Promoting	Promoting

7.5 ATR-FTIR

The FTIR was applied for the feather samples as it can provide information about the chemical structure and more specifically about the secondary structures of proteins. The FTIR spectra of the ground samples (Figure 13) contain characteristic absorption bands mainly assigned to vibration of peptide bonds (CONH) in the polypeptide backbone. The band at 1600-1700 cm^{-1} is mainly attributed to the C=O stretching vibration, and is known as Amide I band. The Amide I vibration is barely affected by side chain vibrations but rather by the secondary structure of the backbone. Thus, the Amide I vibration is suitable for secondary structure analysis. The band at 1480-1570 cm^{-1} originates from Amide II structure. This band is resulted from out-of-phase combination of NH bending and CH stretching vibration. Like Amide I vibrations, also Amide II band is more depended on the secondary structure of the protein than the nature of the side chains. The band arisen at 1200-1300 cm^{-1} is attributed mostly to in-phase combination of NH bending and CN stretching vibrations, and it is called Amide III. Amide III vibration depends also on the side chains which makes it more complex to analyze. However, also Amide III band can be used to analyze the secondary structure of the protein. Additionally, the band at approximately at 3300 cm^{-1} is called Amide A band, and hydrogen bonded NH stretching gives rise to it. This band is insensitive to the conformation of the polypeptide backbone but its frequency depends rather on the strength of the hydrogen bonding. (Barth, 2007) The characteristics bands at 2850-2930 cm^{-1} are mostly due to alkyl CH stretch (Bower & Maddams, 1992). In general, when FTIR peaks are compared with each other, it can be assumed that new interactions have taken place if the peaks have shifted in other direction or if the peaks have broaden.

The FTIR spectra (Figure 13) for all samples are relative similar which indicates that they are all keratin and there are no major differences in the chemical structures. However, some differences can be seen. First of all, some differences can be observed in the alkyl CH stretching region at 2850-2920 cm^{-1}. It can be observed that the rachis and regenerated keratin have lower peak intensity compared to other samples. The alkyl CH stretching is most probably due to the side chains in amino acids or hydrocarbon chains in lipids. Conspicuous difference can be also seen at 1743 cm^{-1} (Figure 13). The intensity of this peak is notably lower for rachis and regenerated keratin compared to other samples. It has been stated that the carboxyl groups without hydrogen bonding give the band above 1740 cm^{-1} (Barth, 2007). The band at 1743 cm^{-1} is suggested to arise due to stretching of ester C=O groups

(Jackson & Mantsch, 1995). More specifically, in the study of Selmin et al. (2012) the band at 1740 cm^{-1} was assigned to lipid ester carbonyl stretching. This suggests that in the barbs and steam exploded feathers there are lipids, fat, present in the structure. This could also explain the higher intensity of the bands at the alkyl CH stretching region for barbs and steam exploded feathers compared to the rachis and regenerated keratin. It has been also suggested that the intensity of CH stretching band at 2850 cm^{-1} decreases as the crystallinity of the sample increases (Bower & Maddams, 1992). This could suggest that the rachis and regenerated keratin have higher content of crystallinity compared to the other samples. However, this conclusion has to be treated with extra caution as the observation between the relation in the band intensity and crystallinity was done for polymer polyvinyl chloride (Bower & Maddams, 1992).

As already mentioned, the Amide I-III bands can be used to predict the secondary structure of the protein. Especially, Amide I-II are useful as they should be less affected by the nature of the side chains, and the vibration of the polypeptide backbone is based on the environment (Barth, 2007). The band positions of different secondary structures have been collected from literature, and they are presented in Table 5.

When the differences between the Amide I-II bands of the processed feathers and the native feathers are compared, some differences can be seen (Figure 13). First of all, it has been stated that unordered structure exhibits a featureless broad amide I band near 1650 cm^{-1} (Barth, 2007). From the spectra, it can be observed that the Amide I bands of steam exploded feathers and regenerated keratin are broadened, and the peak maxima have shifted towards higher wavenumbers. Secondly, the steam exploded feathers show sharp maximum at 1538 cm^{-1} while regenerated keratin shows sharp maximum at 1514 cm^{-1} in the Amide II bands.

The Amide I-II bands of the native feather samples (Figure 13) have relatively similar shapes with each other showing slight differences. In order to determine the overlapping bands and observe the differences in Amide I-II bands, deconvolution of these bands in their individual components was carried out according to the studies of Tsuboi et al. (1991) and Rintoul et al. (2000) (Appendix 1). The peaks were assigned according to Table 5, and the results are summarized in Table 6. It has to be noted that the results obtained from deconvolution have always to be treated with caution as the deconvolution process include a lot of parameters and choosing the

right parameters is rather subjective (Jackson & Mantsch, 1995). However, based on the deconvoluted spectra the whole feather and rachis contain more antiparallel β-sheet and turns than barbs which have more α-helix as well as random coil (Table 6).

The deconvolution was also carried out for processed feathers (Table 6 & appendix 1). However, the obtained peak positions varied from the peak positions obtained for native feathers, and peak assigning was not as clear. This could indicate that the environment and secondary structure of the polypeptide backbone have changed, and results have to be interpreted with caution. The results obtained from the deconvolution, nevertheless, indicate that the steam explosion degraded the β-sheet structure and increased the portion of α-helix and random coil while the DES extraction and regeneration retained the content of β-sheet but destroyed the α-helix as well as increased the content of random coil. Moreover, it is assumed that the antiparallel β-sheet in native feather changed, at least partly, to parallel β-sheet in regenerated keratin as the peak maximum moved towards higher wavenumbers (Barth 2007 & Appendix 1).

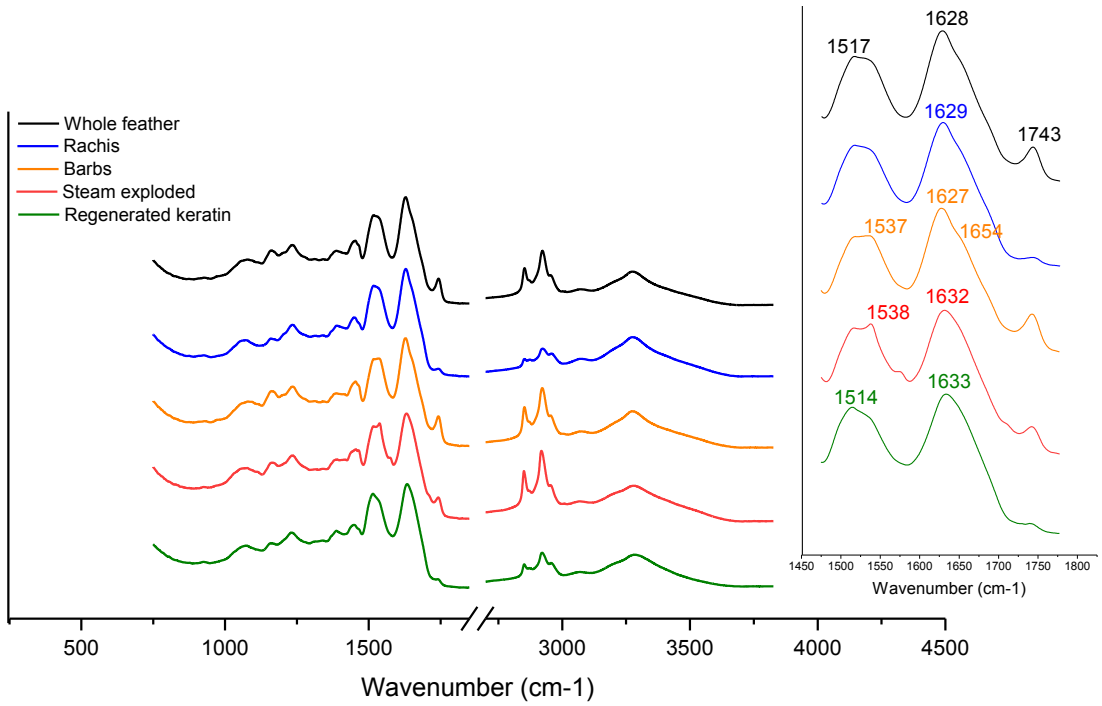

Figure 13. FTIR spectra of ground whole feather, rachis, and barbs (a) as well as of whole feather, steam exploded feathers, and regenerated keratin (b).

Table 5. The different band positions assigned to the secondary structures of protein.

Band	Position of the secondary structure (cm^{-1})				
	α-helix	β-sheet	Turns	Random coil	Reference
Amide I	1654	1633,1684	1672	1654	(Barth 2007)
	1650	1630	-	1660	(Miyazawa & Blout 1961)
	-	1630	-	1650	(Ha et al. 2005)
Amide II	-	-	1520	1535	(Miyazawa & Blout 1961)
	-	-	1520	1540	(Ha et al. 2005)
Amide III	-	-	1270	1230	(Ha et al. 2005)

Table 6. Summary of ATR-FTIR deconvolution.

Sample	α-helix + random coil (%)	β-sheet (%)	Turns (%)	Random coil (%)
Whole feather	6.4	34.0	16.3	43.3
Rachis	6.0	34.7	17.1	42.2
Barbs	12.6	26.6	10.2	50.5
Steam exploded	21.9	15.9	9.4	52.9
Regenerated keratin	4.2	33.0	13.9	48.8

7.6 Raman spectroscopy

Raman spectroscopy is a useful technique which can provide information about the protein structure and conformation as well as about the orientation of the protein chains. Visible light Raman was applied for sectioned rachis and barbs as it enables the specific localization of the measurement position. This way the measurement could be selectively targeted to the outer layer and honeycomb structure separately. In sectioned barbs sample it was also possible to target in the barbule structure. The collected spectra and the measurement positions are presented in Figure 14. The processed feathers could not be measured with this technique as they were emitted strong background that overwhelmed the Raman scattering.

The spectra obtained from different sectioned samples (Figure 14) were quite similar with slight differences. The most noticeable differences were between the spectra of outer layers and the inner honeycomb structures and their band intensities. Additionally, the spectrum of barbule is something between the outer layers and honeycomb structures. Like in IR, also in Raman spectra the most characteristics bands were assigned to peptide bonds (COHN). However, In Raman, when determining the protein secondary structure, especially Amide I and III vibrations of the peptide groups are beneficial. (Rygula et al., 2013) Amide I is the stretching vibration of the C=O bond in the polypeptide backbone at 1600-1690 cm^{-1} (Rygula et al., 2013). Amide I band arises the band maximum at ca. 1650 cm^{-1} when in α-helix while the band maximum in antiparallel β-sheet and β-turn takes place at ca. 1670

cm^{-1} (Schmidt & Jayasundera, 2003). On the other hand, in amide III, which is due to coupled CH stretching and NH bending vibrations and which occurs at 1230-1300 cm^{-1} (Rygula et al., 2013), it has been suggested that the band at ca. 1241 cm^{-1} is assigned for β-sheet while the band at 1280 cm^{-1} is assigned to β-turn (Church et al., 2010) and/or to α-helix (Edwards et al., 1998). Besides the bands arisen from peptide bonds, there are a range of other features present in Raman spectra. These bands are mainly due to amino acid side chains or to sulphur containing residues (Rygula et al., 2013). Moreover, the strong peaks arisen in the region of 2800-3100 cm^{-1} is assigned for CH stretching due to CH, CH_2, and CH_3 groups in side chains. In the analysis, it should be taken in to account that the bands from different amino acids do not have an exact locations in the spectra as the molecular interactions cause variation to the Raman shifts. For example, there is a decrease in the Raman shift for hydrogen bonded group compared to the free functional group. (Howell et al., 1999)

When outer layers of rachis and barbs are compared to their honeycomb structures, Amide I band at ca. 1669 cm^{-1} was stronger in outer layers than in the inner honeycomb structures (Figure 14). In the honeycomb structures as well as in the barbule these bands are broadened towards higher wavenumbers. This broadening suggests that wider range of conformations and orientation may be present in the honeycomb structure (Church et al., 2010). It has been stated that in crystals, molecules are in an exact place within a regular structure which produces a very sharp peaks whereas the randomness causes peak bordering. This effect is especially observed when spectra of solids and liquids are compared. (Zhu et al., 2011) It can be assumed that honeycomb structures, indeed, are not as ordered as outer layers. Another explanations for the band broadening in honeycomb structures as well as in the barbule could be other structures such as lipids.

In order to determine the overlapping peaks in the Amide I band, deconvolution was carried out. This was done only for outer layers as the broadening of the band in honeycomb structure and in barbule made the fitting impossible. Peak fitting and assigning were done according to the studies of Schmidt & Jayasundera (2003) and Rintoul et al. (2000) (Appendix 2). The results of the deconvolution (Table 7) indicate that the outer layer of barbs is richer in α-helix and slightly richer in other structures (Asp, Glu, aromatic amino acids) while rachis consist mainly β-sheet and disordered structure. Additionally, the Amide III bands of samples (Figure 14) indicate that the outer layer of rachis has more β-sheet than β-turn and α-helix as the there is a peak

at 1245 cm^{-1} but no clear peak at 1280 cm^{-1} (Church et al., 2010; Edwards et al., 1998). In all other samples peak at 1280 cm^{-1} can be observed. The different levels of the band broadness could also indicate to different ranges of conformations. These results agree with the results obtained from FTIR (Table 6). However, slight differences in the accurate percentages can be observed. For example, Raman studies give higher content of α-helix than FTIR. This is most probably explained by the obscurity of the deconvolution process. Also, in FTIR studies the samples were ground which means that also honeycomb structure is included to the results. Thus, results obtained from deconvolution have to be treated with caution.

The band at ca. 1690 cm^{-1} which was able to be determined after deconvolution, is assigned to side chain carbonyl groups of Asp and Glu (Rintoul et al., 2000). The small broad bands at approximately 1610 cm^{-1} seen in Amide I bands of different structural parts of barbs and of barbule are probably due to vibrations of aromatic amino acids (Chi et al., 1998). In feathers, this band may indicate to the vibration of the C=C bond in the aromatic ring of Tyr or Phe (Barone et al., 2006). Phe is also suggested to have band at 1031 cm^{-1} and the Phe ring mode at around 1002-1005 cm^{-1} (Rygula et al., 2013).

The band at 522 cm^{-1} is most probably assigned to S-S bond and more specifically to *gauche–gauche–trans* conformation (Edwards et al., 1998). This band can be seen in every sample (Figure 14), especially in the outer layer of rachis, barbs and barbule, and the intensity seems to greatest at the band in the outer layer of barbs. All the conformations of S-S bond are suggested to be located in the region of 490-550 cm^{-1} (Edwards et al., 1998) which indicates that the sample with broader bands in this area has wider range of S-S conformations. From the spectra (Figure 14) it could then be assumed that the S-S bonds in outer layers as well as in the barbule are more uniform in the conformation and orientation compared to honeycomb structures.

The bands at 605 cm^{-1} and 830-900 cm^{-1} could indicate to the wagging of CH groups and more specifically to the vibration of CCH and CH groups, respectively (Edwards et al., 1998). Moreover, the stretching region at approximately 2800-3100 cm^{-1} is assigned for CH stretching in the groups in side chains and in lipids (Howell et al., 1999). From the spectra of the samples (Figure 14) it can be seen that the peak at 605 cm^{-1} as well as the peaks at 830-900 cm^{-1} are present in all samples, expected the outer layer of the rachis. They have also quite low intensity in the outer layer of the barbs. Also, the intensity of the peaks at the region of 2800-3100 cm^{-1} is weakest

to the outer layer of the rachis while greatest to the honeycomb structure of the rachis and to the barbule. Based on the assumption that the free groups give increased Raman shift (Howell et al., 1999), it could be suggested that the in the honeycomb structures in the barbule there are more free groups and mobility. This could indicate that there is less crystallinity in the honeycomb structures compared to the outer layers. The higher intensities, could also indicate to the presence of lipids like was discussed in FTIR section.

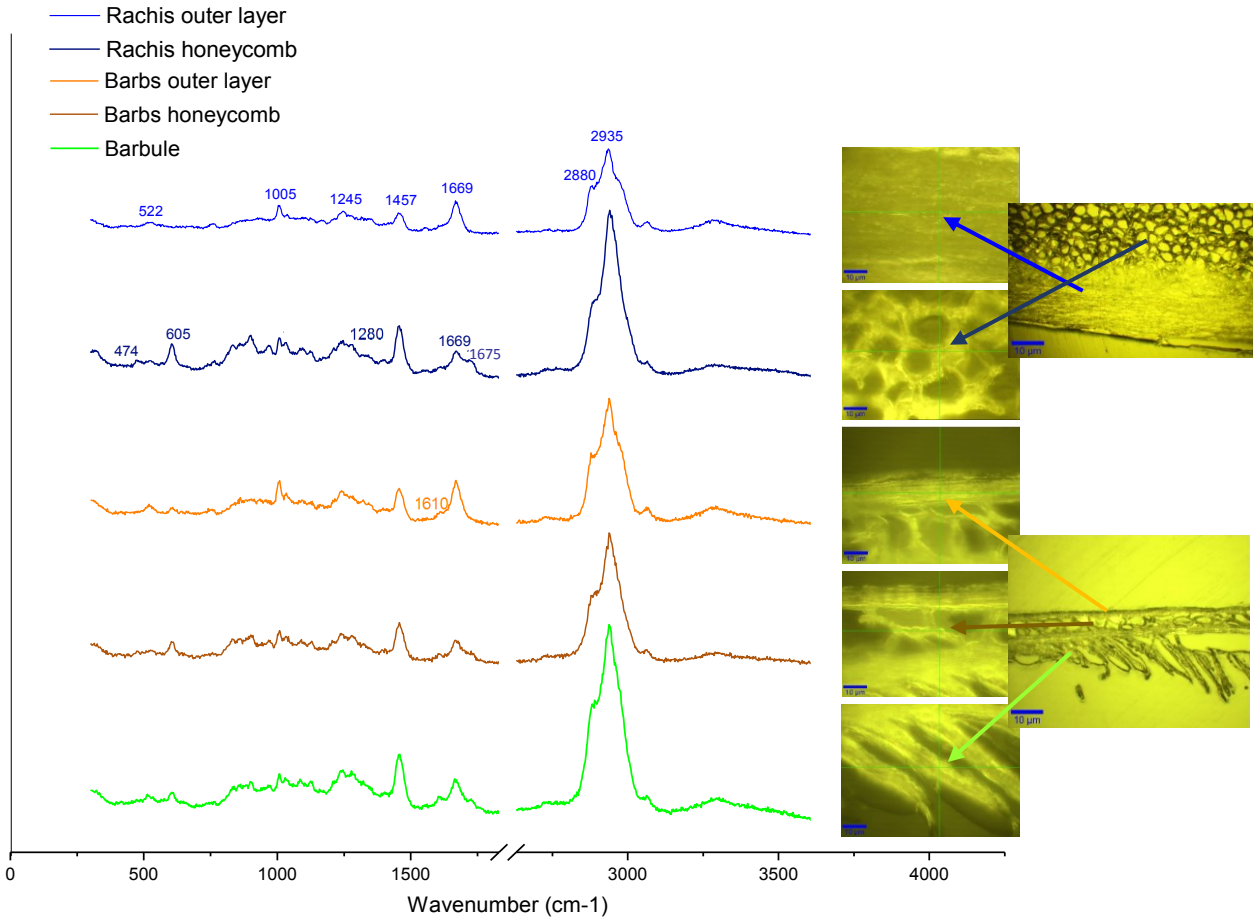

Figure 14. Raman spectra and targeted measurement points of the outer layer of rachis, the honeycomb structure of rachis, the outer layer of barb, the honeycomb structure of barb and the barbule.

Table 7. Summary of Raman deconvolution.

Outer layer	α-helix (%)	β-sheet + disordered (%)	other (%)
Rachis	15.1	47.9	37.9
Barbs	23.7	33.7	42.6

Besides the compositional information, polarized Raman spectroscopy can be used to determine the orientations of the molecules within the sample. This can be done by measuring the isotropic and anisotropic responses of the sample to different polarized radiation. (E. Smith & Dent, 2005) Rintoul et al. (2000) have observed that feather barbule show considerable dichroism for many bands from which Amide I band can be used to interpret the orientation of the β-sheet structure. Also, Tsuboi et al. (2006), have studied the polarized Raman spectra of the feather rachis in the Amide I band.

In this study, the polarized Raman spectra was collected keeping the sample in the fixed position and varying the polarization angle of the laser beam between 0° and 90°. Although, many bands showed anisotropic response, Amide I band was utilized to summarize the results (Figure 15). From the results, it can be seen that in the outer layers (Figure 15a&c) the intensity of Amide I bands are greatest at θ = 60–90°. At θ = 0–30°, the band intensities decrease. This means that when the polarization of the laser is parallel to the fiber axis, the stretching vibration of the C=O bonds in the polypeptide backbone give highest intensity. This, on the other hand, could indicate that the most of the bonds are oriented in the axial direction and supports the hypothesis of fibrous structure. It could be assumed that chains in β-sheet and α-helix are axially oriented while β-turn and random coil are not oriented unidirectional (Tsuboi et al., 2006). The intensities of Amide I bands in honeycomb structures (Figure 15b&d) suggest the chains in honeycomb structure are rather disorganized than oriented in one specific direction. In the study of Rintoul et al. (2000), the β-sheet structure was found to be oriented between the θ = 60–90°. However, they noted that due to complexity of the biological material, there is a need for caution when protein orientation is determined using vibrational spectroscopic methods, and use of Raman intensities, the unique orientation of the feather barbule could not be determined. (Rintoul et al., 2000)

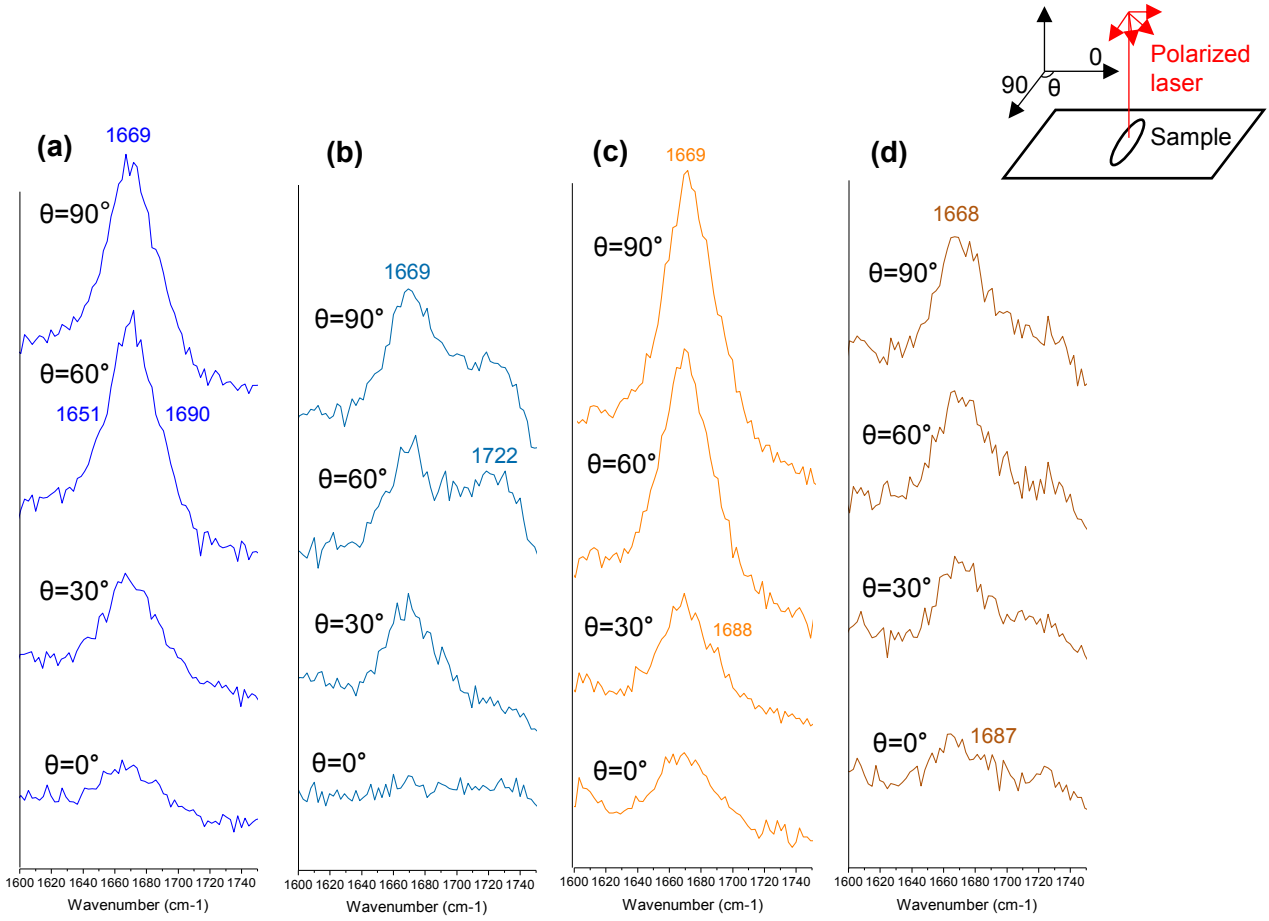

Figure 15. Polarized Raman spectra obtained from the outer layer of rachis (a), honeycomb structure of rachis (b), outer layer of barb (c), and honeycomb structure of barb (d).

7.7 XRD

XRD was used to determine the crystallinity in the ground samples. The patterns obtained (Figure 16) clearly indicate all of the samples are semi crystalline keratin with peaks at approximately 9° and 20° corresponding to the crystalline spacing of 9.8 Å and 4.4 Å, respectively (Reddy & Yang, 2007; Xu et al., 2014). From the patterns, it can be seen that the rachis produce sharpest peaks with the highest peak intensities. This could indicate higher content of crystallinity compared to the other samples (Reddy & Yang, 2007). The diffraction patterns of whole feather and barbs are very similar, whole feather having a bit higher intensity of the peak at 20°. From the diffraction patterns of processed feathers, it can be observed that the peaks are broader than the ones of native feathers. The peak intensities of regenerated keratin are greater than the intensities of steam exploded feathers. The decrease in the

intensities of the peaks could indicate the lower content of crystalline structures (Khosa et al., 2013) while different spacing as well as peak positions may indicate different crystal structures and different arrangements of crystals (Reddy & Yang, 2007).

For all diffraction patterns, deconvolution was carried out according to the study of Cao & Billows (1999), and using Lorentz fit as it gave better cumulative peak fit compared to Gaussian fit (Appendix 3). The results obtained from the deconvolution (Table 8), indicates that the degree of the crystallinity in native feathers is highest in the rachis, second highest in the whole feather and lowest in the barbs. The study of Reddy & Yang (2007) also reported that the degree of crystallinity is higher in the rachis compared to the barbs. However, the obtained degree of crystallinity (61.9 %) is incompatible as in their study the crystallinity of barbs was reported to be 24.8 %. Nevertheless, it has also been reported already in 1971 that feather keratin has very high degree of crystallinity compared to other fibrous proteins (Fraser et al., 1971). When result obtained from the deconvolution are compared between the whole feather and processed feathers, it can be observed that in the regenerated keratin the crystallinity remains similar while in the steam exploded feathers it decreases a bit. Thus, it is suggested that relatively efficient recrystallization has taken place in the regeneration process although from the elemental analysis and amino acid content it was interpreted that the content disulfide crosslinking has been partly destroyed (Table 1 & 3). On the other hand, the steam explosion is assumed to disturb the ordered structure. It is also important to notice that the crystalline peaks in processed feather are broader than in the native feather (Appendix 3) which indicate that the crystalline structure and arrangement is different (Reddy & Yang, 2007).

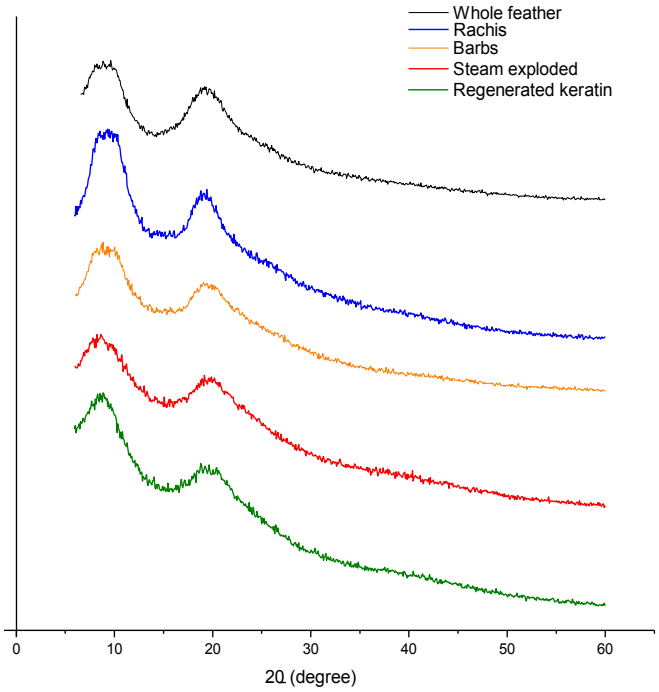

Figure 16. XRD patterns of ground feather samples.

Table 8. Summary of XRD deconvolution.

Sample	Crystallinity (%)	Amorphous (%)
Whole feather	65.8	34.2
Rachis	71.2	28.8
Barbs	61.9	38.1
Steam exploded	60.2	39.8
Regenerated keratin	64.6	35.4

7.8 Solid-state NMR

Solid-state ^{13}C NMR spectroscopy was used to investigate the molecular conformation and molecular dynamics of the ground feather samples. From the obtained results (Figure 17), it can be seen that the spectra for the ground samples are similar with slight differences in the intensities. It can also be observed that the spectra are characteristics for the feather keratin (Idris et al., 2013). It has to be noted that, NMR is not widely applied technique to understand the biological conformations due to the difficulties in understanding the link between the chemical shifts and structural parameters (Pelton & Mclean, 2000). However, some attempts have been carried out to investigate the molecular structures and dynamics of keratin, for

example, by Duer et al. (2003), Carr & Gerasimowicz (1988) and Nishikawa et al. (1998).

First of all, the peaks seen at 171 ppm are assigned for carbonyl carbons (Duer et al., 2003) while peaks at approximately 130 ppm are due to aromatic species (Carr & Gerasimowicz, 1988). The regions of 35-10 ppm are due to alkyl compounds of the side chains (Duer et al., 2003). The peaks at 59 ppm are ascribed to α-carbon while the smaller peak at 69 ppm seen in barbs is suggested to be assigned for β-carbon in amino acid residue Thr (Duer et al., 2003). According to the amino acid content (Table 3), barbs contain slightly more Thr. The peak observed at 54 ppm in the whole feather and barbs but not in the rachis could be due to α-carbon in amino acid residues Glu, Arg and Leu which are located in β-sheet or in random coil. Based on the amino acid content (Table 3), the content of Glu and Arg is higher in the whole feather and barbs while Leu is richer in the rachis. The peak at 41 ppm is suggested to be assigned for β-carbon in Leu and in crosslinked Cys. In turn, Cys which is not crosslinked and include thiol groups give a β-carbon signal at 25-29 ppm. (Duer et al., 2003) However, this peak is difficult to differentiate from the peaks assigned to the alkyl side chains at the same region. From the spectra (Figure 17), it can be seen that the rachis give slightly higher peak at 41 ppm than the barbs and the whole feather when the intensity of the peak is compared to the intensity of the peak at 38 ppm. This could indicate that the rachis has higher content of Leu and/or crosslinked Cys. The other peaks at the region of 32-40 ppm are ascribed for Glu and Pro (Duer et al., 2003). Moreover, in processed feathers, the largest differences compared to the native feathers can be seen in the intensity of the α-carbon peak.

As could been seen from the above, the peak assigning and interpreting based on the spectra were complex due to different amino acid residues and did not really give any concrete information. This is why, deconvolution for the peak arisen from the carbonyl carbons is carried out. The carbonyl groups of amino acid residues give slightly different shift depending whether it is located in α-helix or β-sheet. In general, carbonyl groups in α-helix have shift at higher ppm compared to carbonyl groups in β-sheet. (Duer et al., 2003) In order to detect the overlapping peaks and different secondary structures in the peak at 171 ppm, deconvolution was carried out. The peaks were assigned according to the studies of Duer et al. (2003), Nishikawa et al. (1998) and Idris et al. (2013) which means that the peak at approximately 175 ppm is assigned to α-helix while peak at 171 ppm is assigned to β-sheet and random coil

(Appendix 4). The results from deconvolution (Table 9) indicate that all samples are richer in β-sheet and random coil than in α-helix. However, when barbs and rachis are compared, it can be seen that the content of α-helix is greater in the rachis than in the barbs. This result is inconsistent with the results obtained from FTIR and Raman. Moreover, the content α-helix in the whole feather is less than in the rachis and barbs while logically thinking it should be something between. Also, the regenerated keratin is not in line with the results obtained from FTIR.

It is important to notice that the carbonyl groups in different amino acid residues give different shifts (Duer et al., 2003) which suggests that, besides the secondary structure, also the nature of the side chains have an effect to the atomic nuclei's ability to absorb and emit electromagnetic radiation. This could also have an effect to the deconvolution process. For example Leu, which is a lot richer in the rachis compared to the barbs and whole feather (Table 3), is suggested to produce shift at 175.5 ppm when it is in β-sheet and at 178.5 ppm when it is in α-helix (Duer et al., 2003). This, on the other hand, could cause broadening of the C=O peak in rachis towards larger shifts, and this way distort the results obtained from the deconvolution. In comparison, in FTIR and Raman, it has been stated that the side chains should not have significant effect to the vibration of the polypeptide backbone in Amide I band (Barth, 2007; Lefèvre et al., 2007). Moreover, it has been stated that when protein's secondary structure is determined by NMR, assigning of the specific amino acid residues is necessary (Pelton & Mclean, 2000). This, on the other hand, will make the determination too complex and time consuming to be included to this master's thesis. It is also important to notice that the samples were ground which means that also honeycomb structure was included to the characterization, and in Raman studies it was suggested that in honeycomb structure the range of conformations is not that uniform. All in all, it seems that the interpretation of the NMR spectra is complex due to its sensitivity for the different amino acid residues and their side chains. In order to understand the spectra, more research and dedication are required.

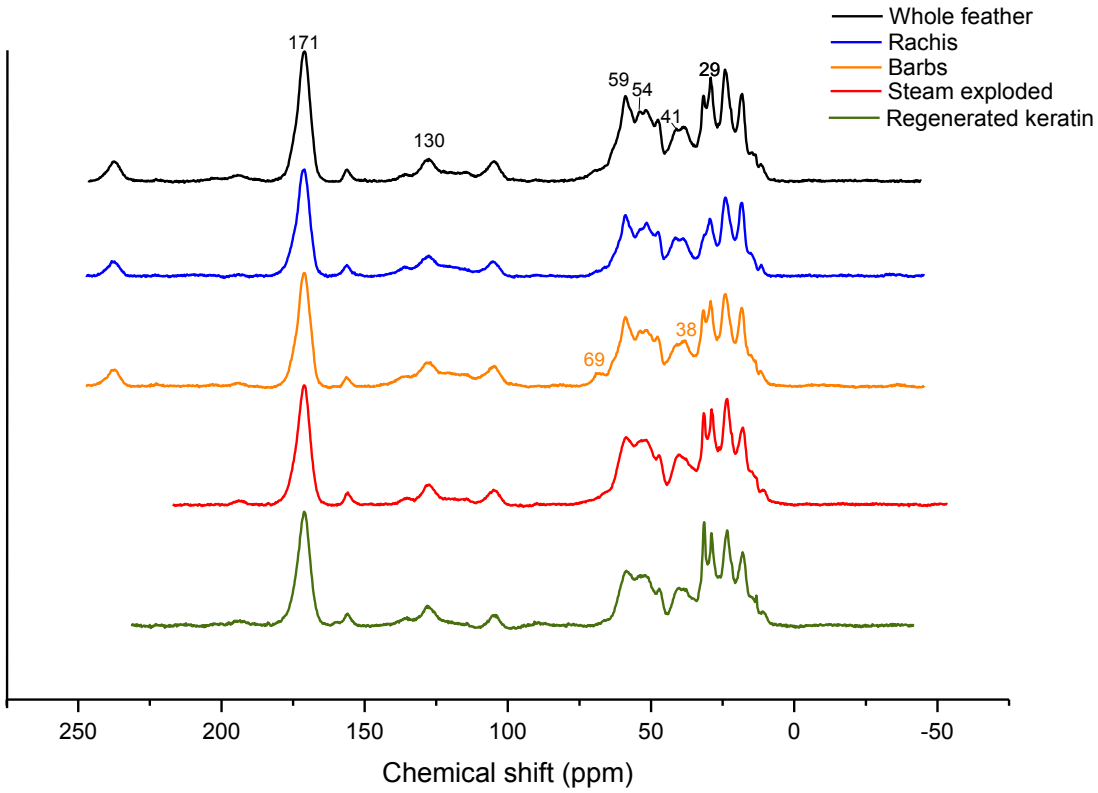

Figure 17. The NMR spectra of ground feather samples.

Table 9. Summary of NMR deconvolution.

Sample	α-helix (%)	Random coil + β-sheet (%)
Whole feather	10.6	89.4
Rachis	17.2	82.9
Barbs	11.2	88.8
Steam exploded	16.7	83.3
Regenerated keratin	14.7	85.3

8 Conclusion

Poultry feathers, one of the most unique industrial coproducts, have shown potential to be further utilized in various applications. In order to realize the full potential of the feathers and their suitability and behavior in different applications, deeper understanding of the correlation between the macro properties and the structures and the dynamics at the molecular level is necessary. In this master's thesis, the different structural parts in native chicken feathers were characterized using various techniques, and the aim was to validate the best characterization techniques for feather keratin. The focus was especially on the characterization of the secondary

structures. Feathers were also processed by two environmentally friendly processing methods which were steam explosion and extraction with deep eutectic solvents. Characterization of these processed feathers was also carried out.

The feather is composed of rachis in which barbs and barbules are attached. It was found that rachis and barbs are built from the fibre like outer layer and the inner honeycomb structure. It is assumed that the outer layer provides protection and support while the honeycomb structure provides the light weight and low density. The results obtained clearly indicated that the feathers are mostly composed of protein called keratin. It is assumed that the feather keratin is a fibrous protein and feathers have a fibrous structure in which crystalline axially oriented microfibrils are embedded in an amorphous protein matrix. In the Raman studies (and partly in microscopy studies), it was observed that this could be the case for the outer layers while the inner honeycomb structure is suggested to have a larger range of conformations and orientations of the polypeptide chains. In the Raman studies, it is also observed that the side chains in the amino acid residues in honeycomb structures had higher mobility. Based on these results, it is assumed that the honeycomb structure is rather amorphous than highly crystalline.

The FTIR and Raman studies indicated that the rachis contains more antiparallel β-sheet while barbs is suggested to have more α-helix and random coil. It has been commonly stated that β-keratin which consists mostly from β-sheet is tougher than the α-keratin which is rich in α-helix. From the FTIR spectra, it was also noticed that the barbs have a higher fat content compared to the rachis. The results from XRD suggested that the crystallinity in rachis is higher than in barbs. Based on the degree of crystallinity and on the higher content of β-sheet structure, it is assumed that rachis is tougher than barbs. From the microscopy images, it was also noticed that the outer layer of the rachis is a lot thicker than in the barbs. These results together could indicate that in the feather, the rachis and the barbs have different functions; rachis provides the structural support while barbs form the flexible protective layer. Furthermore, it was observed that the results from NMR were inconsistent with the results obtained from FTIR and Raman. Additionally, no clear conclusions were able to be drawn from the NMR spectra. It was observed that the carbon nuclei in the similar bonds but in different amino acid residues cause slightly different shifts which make the results complex to be interpreted at this thesis. In comparison, the band

positions in FTIR and Raman spectra, are rather depended on the conformation of the backbone chain than the side chains.

The feathers were successfully steam exploded as well as dissolved and regenerated in deep eutectic solvent. From the microscopy images, it was seen that the processed feathers were composed rather of uniform matrix than of different structural parts. Based on the elemental analysis the content of sulphur in processed feathers decreased remarkably compared to the native feathers. Also, the cysteine content was the lowest for the processed feathers according to the amino acid analysis. These results together indicate that also the disulfide crosslinking has been partly destroyed. It has been stated that the disulfide crosslinks play an important role in the hardness of the material. However, it has been also observed that the part of the polypeptide chain which is concentrated in cysteine residues was almost missing the ordered secondary structure.

From the FTIR results, it was observed that after the steam explosion, the ordered structure changed. It is suggested that, compared to the native feathers, the content of β-sheet decreased while the content of α-helix and random coil increased. The FTIR results also indicated that there is fat present in the structure. The XRD results indicated that the crystallinity in steam exploded feathers has decreased compared to the native feathers. Based on the XRD patterns, it is also suggested that the crystalline structure is different and there is a wider range of crystal arrangements present.

In comparison to the steam explosion, the FTIR results for regenerated keratin indicated that the content of β-sheet remained approximately the same while α-helix seemed to decrease and random coil, again, increase compared to the native feather. It is also suggested that the conformation of β-sheet is slightly different. Moreover, there was no fat observed in the structure. The XRD study suggests that the degree of crystallinity in regenerated keratin is similar with the native feathers. However, it seems that the crystal structure is different as well as has a wider range of arrangements. All in all, although the disulfide crosslinking has been partly destroyed, recrystallization has taken place in regenerated keratin. However, the lack of these crosslinking partly explains the different conformation the polypeptide chains and crystal arrangements.

From applied characterization methods Raman spectroscopy provided valuable information in the characterization of native feathers while optical microscopy, FTIR,

and XRD were beneficial and informative in the characterization of both, native and processed feathers. As a simple and fast method, also, elemental analysis could provide added value for the characterization process of processed feathers. However, in that case, the correlation between the elemental content and the changes taking place in the chemical structure during the specific processing has to be clear. In order to apply NMR as the characterization method for the feathers, more research is required. Moreover, due to extensive processing protocol, amino acid analysis is not suggested to characterize the feathers which are further utilized in material applications. For future studies, it is suggested that the MALDI-TOF MS, which is used to determine the molecular weight, could provide valuable information of the polypeptide chain degradation during the processing. Also, in order to visualize the fibrous structure of the feathers, SEM and TEM are recommended. These techniques were excluded from this thesis as the focus was kept on the secondary structure. Moreover, other characterization techniques should be chosen based on the chosen application and which properties are important.

To summarize, in this Master's thesis, some structures and dynamics at the molecular level of the feathers have been characterized and identified, especially focusing on the secondary structure. This was done by using various characterization techniques from which optical microscopy, FTIR, Raman spectroscopy, and XRD were found to be the most valuable ones. The differences in the chemical structure and composition between the different structural parts of the native feathers were found and discussed. It was also observed that the processing of the feathers changed the structures and dynamics, and the different processing method had a different effect. It is then suggested that by varying the processing method and conditions, different macro properties for the end product can be optimized.

9 References

Abbott, A. P., Boothby, D., Capper, G., Davies, D. L., & Rasheed, R. K. (2004). Deep eutectic solvents formed between choline chloride and carboxylic acids: versatile alternatives to ionic liquids. *Journal of the American Chemical Society*, 126(29), 9142-9147.

Aguayo-Villarreal, I. A., Bonilla-Petriciolet, A., Hernández-Montoya, V., Montes-Morán, M. A., & Reynel-Avila, H. E. (2011). Batch and column studies of Zn 2+ removal from aqueous solution using chicken feathers as sorbents. *Chemical Engineering Journal*, 167(1), 67-76.

Alberts, B., Bray, D., Lewis, J., Raff, M., Roberts, K., Watson, J. D. (1994). *Molecular Biology of the Cell [e-book]*. Taylor & Francis. From <http://www.myilibrary.com?ID=34866>

Alger, M. (1996). *Polymer science dictionary* (2nd ed.). London: Chapman & Hall.

Anonymous. (2005). 2.2.56. Amino Acid Analysis. In *European Pharmacopoeia 5.0 [PDF document]*. From <https://www.researchgate.net/file.PostFileLoader.html?id=526583ecd3df3e1d16cc0bf7&assetKey=AS%3A272155265175554%401441898279550>

Arai, K. M., Takahashi, R., Yokote, Y., & Akahane, K. (1983). Amino-Acid Sequence of Feather Keratin from Fowl. *The FEBS Journal*, 132(3), 501-507.

Barone, J. R., & Schmidt, W. F. (2005). Polyethylene reinforced with keratin fibers obtained from chicken feathers. *Composites Science and Technology*, *65*(2), 173-181.

Barone, J. R., Schmidt, W. F., & Gregoire, N. T. (2006). Extrusion of feather keratin. *Journal of applied polymer science*, *100*(2), 1432-1442.

Barone, J. R., Schmidt, W. F., & Liebner, C. F. (2005). Thermally processed keratin films. *Journal of applied polymer science*, *97*(4), 1644-1651.

Barth, A. (2007). Infrared spectroscopy of proteins. *Biochimica et Biophysica Acta - Bioenergetics*, *1767*(9), 1073–1101.

Belarmino, D. D., Ladchumananandasivam, R., Belarmino, L. D., Pimentel, J. R. D. M., da Rocha, B. G., Galvão, A. O., & de Andrade, S. M. (2012). Physical and morphological structure of chicken feathers (keratin biofiber) in natural, chemically and thermally modified forms. *Materials Sciences and Applications*, *3*(12), 887.

Benesch, R. (Ed.). (2012). *Sulfur in proteins*. London: Academic Press INC.

Bower, D. I., & Maddams, W. F. (1992). *The vibrational spectroscopy of polymers*. Cambridge: Cambridge University Press.

Cao, J., & Billows, C. A. (1999). Crystallinity determination of native and stretched wool by X-ray diffraction. *Polymer International*, *48*(10), 1027-1033.

Carr, C. M., & Gerasimowicz, W. V. (1988). A Carbon-13 CPMAS Solid State NMR Spectroscopic Study of Wool: Effects of Heat and Chrome Mordanting. *Textile Research Journal*, *58*(7), 418-421.

Chi, Z., Chen, X. G., Holtz, J. S., & Asher, S. A. (1998). UV resonance Raman-selective amide vibrational enhancement: quantitative methodology for determining protein secondary structure. *Biochemistry*, *37*(9), 2854-2864.

Chou, P. Y., & Fasman, G. D. (1974). Prediction of protein conformation. *Biochemistry*, *13*(2), 222-245.

Chou, P. Y., & Fasman, G. D. (1978). Empirical predictions of protein conformation. *Annual review of biochemistry*, *47*(1), 251-276.

Church, J. S., Poole, A. J., & Woodhead, A. L. (2010). The Raman analysis of films cast from dissolved feather keratin. *Vibrational Spectroscopy*, *53*(1), 107-111.

Creighton, T. E. (2010). *The physical and chemical basis of molecular biology [e-book]*. Helvetian Press. From <http://app.knovel.com/hotlink/toc/id:kpPCBMB002/physical-chemical-basis/physical-chemical-basis>

Dalev, P. G. (1994). Utilisation of waste feathers from poultry slaughter for production of a protein concentrate. *Bioresource Technology*, *48*(3), 265–267.

Duer, M. J., McDougal, N., & Murray, R. C. (2003). A solid-state NMR study of the structure and molecular mobility of α-keratin. *Physical Chemistry Chemical Physics*, *5*(13), 2894-2899.

Edwards, H. G. M., Hunt, D. E., & Sibley, M. G. (1998). FT-Raman spectroscopic study of keratotic materials: horn, hoof and tortoiseshell. *Spectrochimica Acta Part A: Molecular and Biomolecular Spectroscopy*, *54*(5), 745-757.

Eslahi, N., Hemmatinejad, N., & Dadashian, F. (2014). From Feather Waste to Valuable Nanoparticles. *Particulate Science and Technology*, *32*(3), 242–250.

Faria, P. C. C., Orfao, J. J. M., & Pereira, M. F. R. (2004). Adsorption of anionic and cationic dyes on activated carbons with different surface chemistries. *Water Research*, *38*(8), 2043-2052.

Ferraro, J. R., & Nakamoto, K. (2003). *Introductory raman spectroscopy (2nd ed.)*. San Diego: Academic Press.

Feughelman, M. (2002). Natural protein fibers. *Journal of Applied Polymer Science*, *83*(3), 489-507.

Filshie, B. K., & Rogers, G. E. (1962). An electron microscope study of the fine structure of feather keratin. *The Journal of Cell Biology*, *13*(1), 1-12.

Fraser, R. D. B., MacRae, T. P., Parry, D. A. D., & Suzuki, E. (1971). The structure of feather keratin. *Polymer*, *12*(1), 35-56.

Fraser, R. B., & Parry, D. A. (2008). Molecular packing in the feather keratin filament. *Journal of structural biology*, *162*(1), 1-13.

Fraser, R. B., & Parry, D. A. (2011). The structural basis of the filament-matrix texture in the avian/reptilian group of hard β-keratins. *Journal of structural biology*, *173*(2), 391-405.

Fraser, R. D. B. M. (Ed.). (2012). *Conformation in fibrous proteins and related synthetic polypeptides*. New York: Academic Press.

Fraser, R. D. B., MacRae, T. P., & Rogers, G. E. (1972). *Keratins: their composition, structure, and biosynthesis*. Springfield: Charles C. Thomas.

Fujii, T., & Li, D. (2008). Preparation and properties of protein films and particles from chicken feather. *International Journal of Biological Macromolecules*, *8*(2), 48–55.

Galvis, L., Bertinetto, C. G., Putaux, J. L., Montesanti, N., & Vuorinen, T. (2016). Crystallite orientation maps in starch granules from polarized Raman spectroscopy (PRS) data. *Carbohydrate Polymers*, *154*, 70–76.

Giraldo, L., & Moreno-Piraján, J. C. (2013). Exploring the use of rachis of chicken feathers for hydrogen storage. *Journal of Analytical and Applied Pyrolysis*, *104*, 243–248.

Godfrey, T., & Reichelt, J. (1982). Industrial enzymology: the application of enzymes in industry. New York: Nature Press.

Goormaghtigh, E., Cabiaux, V., & RUYSSCHAERT, J. M. (1990). Secondary structure and dosage of soluble and membrane proteins by attenuated total reflection Fourier-transform infrared spectroscopy on hydrated films. *The FEBS Journal*, *193*(2), 409-420.

Grazziotin, A., Pimentel, F. A., Sangali, S., de Jong, E. V., & Brandelli, A. (2007). Production of feather protein hydrolysate by keratinolytic bacterium Vibrio sp. kr2. *Bioresource Technology*, *98*(16), 3172–3175.

Harrap, B. S., & Woods, E. F. (1964). Soluble derivatives of feather keratin. 1. Isolation, fractionation and amino acid composition. *The Biochemical Journal*, *92*(1), 8–18.

Hillenkamp, F., Karas, M., Beavis, R. C., & Chait, B. T. (1991). Matrix-assisted laser desorption/ionization mass spectrometry of biopolymers. *Analytical Chemistry*, *63*(24), 1193A–1203A.

Ho, W. F., Prichard, E. R., & Stuart, B. (2003). *High performance liquid chromatography*. Cambridge: Royal Society of Chemistry.

Howell, N. K., Arteaga, G., Nakai, S., & Li-Chan, E. C. (1999). Raman spectral analysis in the C-H stretching region of proteins and amino acids for investigation of hydrophobic interactions. *Journal of Agricultural and Food Chemistry*, *47*(3), 924–33.

Hu, C., Reddy, N., Yan, K., & Yang, Y. (2011). Acetylation of chicken feathers for thermoplastic applications. *Journal of Agricultural and Food Chemistry*, *59*(19), 10517–10523.

Huda, S., & Yang, Y. (2008). Composites from ground chicken quill and polypropylene. *Composites Science and Technology*, *68*(3–4), 790–798.

Idris, A., Vijayaraghavan, R., Rana, U. A., Fredericks, D., Patti, a. F., & MacFarlane, D. R. (2013). Dissolution of feather keratin in ionic liquids. *Green Chemistry*, *15*(2), 525.

Jackson, M., & Mantsch, H. H. (1995). The use and misuse of FTIR spectroscopy in the determination of protein structure. *Critical Reviews in Biochemistry and Molecular Biology*, *30*(2), 95–120.

Jamdar, S. N., & Harikumar, P. (2005). Autolytic degradation of chicken intestinal proteins. *Bioresource Technology*, *96*(11), 1276–1284.

Ji, Y., Chen, J., Lv, J., Li, Z., Xing, L., & Ding, S. (2014). Extraction of keratin with ionic liquids from poultry feather. *Separation and Purification Technology*, *132*(2014), 577-583.

Jääskeläinen, A. S., Holopainen-Mantila, U., Tamminen, T., & Vuorinen, T. (2013). Endosperm and aleurone cell structure in barley and wheat as studied by optical and Raman microscopy. *Journal of Cereal Science*, *57*(3), 543–550.

Kammiovirta, K., Jääskeläinen, A.-S., Kuutti, L., Holopainen-Mantila, U., Paananen, A., Suurnäkki, A., & Orelma, H. (2016). Keratin-reinforced cellulose filaments from ionic liquid solutions. *RSC Advances*, *6*(91), 88797–88806.

Khosa, M. A., Wu, J., & Ullah, A. (2013). Chemical modification, characterization, and application of chicken feathers as novel biosorbents. *Rsc Advances*, *3*(43), 20800-20810.

Kwok, D. Y., & Neumann, A. W. (1999). Contact angle measurement and contact angle interpretation. *Advances in colloid and interface science*, *81*(3), 167-249.

Lefèvre, T., Rousseau, M. E., & Pézolet, M. (2007). Protein secondary structure and orientation in silk as revealed by Raman spectromicroscopy. *Biophysical journal*, *92*(8), 2885-2895.

Lingham-Soliar, T., Bonser, R. H. C., & Wesley-Smith, J. (2010). Selective biodegradation of keratin matrix in feather rachis reveals classic bioengineering. *Proceedings of The Royal Society*, *277*(1685), 1161–1168.

Ma, B., Qiao, X., Hou, X., & Yang, Y. (2016). Pure keratin membrane and fibers from chicken feather. *International Journal of Biological Macromolecules*, *89*, 614–621.

Martinez-Hernandez, A. L., Velasco-Santos, C., De Icaza, M., & Castano, V. M. (2005). Microstructural characterisation of keratin fibres from chicken feathers. *International Journal of Environment and Pollution*, *23*(2), 162–178.

Markley, J. L., & Opella, S. J. (Eds.). (1997). *Biological NMR spectroscopy*. New York: Oxford University Press.

McKittrick, J., Chen, P. Y., Bodde, S. G., Yang, W., Novitskaya, E. E., & Meyers, M. A. (2012). The structure, functions, and mechanical properties of keratin. *Jom*, *64*(4), 449-468.

Miyazawa, T., & Blout, E. R. (1961). The Infrared Spectra of Polypeptides in Various Conformations: Amide I and II Bands. *Journal of the American Chemical Society*, *83*(3), 712–719.

Moore, K. E., Mangos, D. N., Slattery, A. D., Raston, C. L., & Boulos, R. A. (2016). Wool deconstruction using a benign eutectic melt. *RSC Advances*, *6*(24), 20095-20101.

Nishikawa, N., Tanizawa, Y., Tanaka, S., Horiguchi, Y., & Asakura, T. (1998). Structural change of keratin protein in human hair by permanent waving treatment. *Polymer*, *39*(16), 3835–3840.

Neil, K. T., & DeGrado, W. F. (1990). A thermodynamic scale for the helix-forming tendencies of the commonly occurring amino acids. *Science*, *250*(4981), 646.

Pauling, L., & Corey, R. (1943). Feather raciiis. *Proceedings of the National Academy of Sciences of the United States of America*, *37*(5), 256–261.

Pedram Rad, Z., Tavanai, H., & Moradi, A. R. (2012). Production of feather keratin nanopowder through electrospraying. *Journal of Aerosol Science*, *51*, 49–56.

Pelton, J. T., & Mclean, L. R. (2000). Spectroscopic Methods for Analysis of Protein Secondary Structure. *Analytical Biochemistry*, *176*(277), 167–176.

Poole, A. J., Church, J. S., & Huson, M. G. (2009). Environmentally sustainable fibers from regenerated protein. *Biomacromolecules*, *10*(1), 1–8.

Poole, A. J., Lyons, R. E., & Church, J. S. (2011). Dissolving Feather Keratin Using Sodium Sulfide for Bio-Polymer Applications. *Journal of Polymers and the Environment*, *19*(4), 995–1004.

Pourjavaheri, F., Jones, O. A., Mohaddes, F., Sherkat, F., Gupta, A., & Shanks, R. A. (2016). Green plastics: Utilizing chicken feather keratin in thermoplastic polyurethane composites to enhance thermo-mechanical properties. In *74th Annual Technical Conference of the Society of Plastics Engineers 2016* (pp. 1-8). Society of Plastics Engineers.

Prum, R. O. (1999). Development and evolutionary origin of feathers. *The Journal of experimental zoology*, *285*(4), 291-306.

Reddy, N. (2015). Non-food industrial applications of poultry feathers. *Waste Management*, *45*, 91–107.

Reddy, N., Hu, C., Yan, K., & Yang, Y. (2011). Thermoplastic films from cyanoethylated chicken feathers. *Materials Science and Engineering: C*, *31*(8), 1706–1710.

Reddy, N., & Yang, Y. (2007). Structure and properties of chicken feather barbs as natural protein fibers. *Journal of Polymers and the Environment*, *15*(2), 81–87.

Rintoul, L., Carter, E. A., Stewart, S. D., & Fredericks, P. M. (2000). Keratin orientation in wool and feathers by polarized Raman spectroscopy. *Biopolymers - Biospectroscopy Section*, *57*(1), 19–28.

Rygula, A., Majzner, K., Marzec, K. M., Kaczor, A., Pilarczyk, M., & Baranska, M. (2013). Raman spectroscopy of proteins: A review. *Journal of Raman Spectroscopy*, *44*(8), 1061–1076.

Saarela, M., Berlin, M., Nygren, H., Lahtinen, P., Honkapää, K., Lantto, R., & Maukonen, J. (2017). Characterization of feather-degrading bacterial populations from birds' nests–Potential strains for biomass production for animal feed. *International Biodeterioration & Biodegradation*, *123*, 262-268.

Saravanan, S., Sameera, D. K., Moorthi, A., & Selvamurugan, N. (2013). Chitosan scaffolds containing chicken feather keratin nanoparticles for bone tissue engineering. *International Journal of Biological Macromolecules*, *62*, 481–486.

Saravanan, K., & Dhurai, B. (2012). Exploration on the amino acid content and morphological structure in chicken feather fiber. *Journal of Textile and Apparel, Technology and Management*, *7*(3).

Sawyer, L. C., Grubb, D. T., & Meyers, G. F. (2008). Applications of Microscopy to Polymers. *Polymer Microscopy*, 248-434.

Schmidt, W. F., & Jayasundera, S. (2004). Microcrystalline avian keratin protein fibers. In *Natural Fibers, Plastics and Composites.* New York: Springer US.

Schor, R., & Krimm, S. (1961). Studies on the Structure of Feather Keratin: I. X-Ray Diffraction Studies and Other Experimental Data. *Biophysical Journal*, *1*(6), 467–487.

Schrooyen, P. M. M., Dijkstra, P. J., Oberthü, R. G., Bantjes, A., & Feijen, J. (2000). Partially carboxymethylated feather keratins. 1. Properties in aqueous systems. *Journal of Agricultural and Food Chemistry*, *48*(9), 4326–4334.

Schrooyen, P. M. M., Dijkstra, P. J., Oberthür, R. C., Bantjes, A., & Feijen, J. (2001). Partially carboxymethylated feather keratins. 2. Thermal and mechanical properties of films. *Journal of Agricultural and Food Chemistry*, *49*(1), 221–230.

Selmin, F., Cilurzo, F., Aluigi, A., Franzè, S., & Minghetti, P. (2012). Regenerated keratin membrane to match the in vitro drug diffusion through human epidermis. *Results in Pharma Sciences*, *2*(1), 72–78.

Senoz, E., Stanzione, J. F., Reno, K. H., Wool, R. P., & Miller, M. E. N. (2013). Pyrolyzed chicken feather fibers for biobased composite reinforcement. *Journal of Applied Polymer Science*, *128*(2), 983–989.

Sharma, S., Gupta, A., Chik, S. M. S. T., Gek, K. C., Podde, P. K., Thraisingam, J., & Subramaniam, M. (2016). Extraction and characterization of keratin from chicken feather waste biomass: a study. In *Proceedings of the national conference for postgraduate research (NCON-PGR 2016), Universiti Malaysia Pahang (UMP), Pekan* (pp. 693-699).

Shi, W., & Dumont, M. J. (2014). Review: Bio-based films from zein, keratin, pea, and rapeseed protein feedstocks. *Journal of Materials Science*, *49*(5), 1915–1930.

Smith, E., & Dent, G. (2013). *Modern Raman spectroscopy: a practical approach*. Chichester: John Wiley & Sons.

Smith, E. L., Abbott, A. P., & Ryder, K. S. (2014). Deep Eutectic Solvents (DESs) and Their Applications. *Chemical Reviews*, *114*(21), 11060–11082.

Striegel, A., Yau, W. W., Kirkland, J. J., & Bly, D. D. (2009). *Modern size-exclusion liquid chromatography: practice of gel permeation and gel filtration chromatography*. Hoboken: John Wiley & Sons.

Sun, P., Liu, Z. T., & Liu, Z. W. (2009). Particles from bird feather: A novel application of an ionic liquid and waste resource. *Journal of Hazardous Materials*, *170*(2–3), 786–790.

Thompson, M. (2008). CHNS Elemental Analysers Report. *AMC Technical Briefs*, *29*.

Tonin, C., Zoccola, M., Aluigi, A., Varesano, A., Montarsolo, A., Vineis, C., & Zimbardi, F. (2006). Study on the conversion of wool keratin by steam explosion. *Biomacromolecules*, *7*(12), 3499–3504.

Tsuboi, M., Kaneuchi, F., Ikeda, T., & Akahane, K. (1991). Infrared and Raman microscopy of fowl feather barb. *NE. Can. J. Chem.*, *69*(1752), 1752–1757.

Tsuboi, M., Kubo, Y., Akahane, K., Benevides, J. M., & Thomas, G. J. (2006). Determination of the amide I Raman tensor for the antiparallel β-sheet: Application to silkworm and spider silks. *Journal of Raman Spectroscopy*, *37*(1–3), 240–247.

Tuna, A., Okumuş, Y., Celebi, H., & Seyhan, A. T. (2015). Thermochemical conversion of poultry chicken feather fibers of different colors into microporous fibers. *Journal of Analytical and Applied Pyrolysis*, *115*, 112-124.

Ullah, A., & Wu, J. (2013). Feather fiber-based thermoplastics: Effects of different plasticizers on material properties. *Macromolecular Materials and Engineering*, *298*(2), 153–162.

USDA (2017). *Livestock and Poultry: World Markets and Trade [PDF documenet]*. From: https://apps.fas.usda.gov/psdonline/circulars/livestock_poultry.pdf. Taken 5.6.2017

Voet, D., & Voet, J. G. (2004). *Biochemistry*. Hoboken: John Wiley & Sons.

Wahlström, R., Kuutti, L., Hiltunen, J., Vuoti, S., Ercili-Cura, D., & Rommi, K. (2017). Process for separating proteins from biomass materials. *WO 2017089655.*

Wang, J., Hao, S., Luo, T., Yang, Q., & Wang, B. (2016). Development of feather keratin nanoparticles and investigation of their hemostatic efficacy. *Materials Science and Engineering C*, *68*, 768–773.

Wang, Q., Cao, Q., Wang, X., Jing, B., Kuang, H., & Zhou, L. (2013). A high-capacity carbon prepared from renewable chicken feather biopolymer for supercapacitors. *Journal of Power Sources*, *225*, 101–107.

Wang, X., Kim, H. J., Wong, C., Vepari, C., Matsumoto, A., & Kaplan, D. L. (2006). Fibrous proteins and tissue engineering. *Materials today*, *9*(12), 44-53.

Wang, Y. X., & Cao, X. J. (2012). Extracting keratin from chicken feathers by using a hydrophobic ionic liquid. *Process biochemistry*, *47*(5), 896-899.

Waseda, Y., Matsubara, E., & Shinoda, K. (2011). X-ray diffraction crystallography: introduction, examples and solved problems. Berlin: Springer Science & Business Media.

Winandy, J. E., Muehl, J. H., Micales, J. A., Agricultural, U., & Orleans, N. (2003). Potential of Chicken Feather Fibre in Wood MDF Composites. In *Proceedings EcoComp 2003, Queen Mary University of London, 1–2 September 2003.*

Wojciechowska, E., Włochowicz, A., & Wesełucha-Birczyńska, A. (1999). Application of Fourier-transform infrared and Raman spectroscopy to study degradation of the wool fiber keratin. *Journal of Molecular Structure*, *511–512*, 307–318.

Woodin, A. M. (1954). Molecular size, shape and aggregation of soluble feather keratin. *Biochemical Journal*, *57*(1), 99.

Xu, H., Shi, Z., Reddy, N., & Yang, Y. (2014). Intrinsically water-stable keratin nanoparticles and their in vivo biodistribution for targeted delivery. *Journal of Agricultural and Food Chemistry*, *62*(37), 9145–9150.

Xu, X., Zhou, Z., & Prum, R. O. (2001). Branched integumental structures in Sinornithosaurus and the origin of feathers. *Nature*, *410*(6825), 200–204.

Yin, X.-C., Li, F.-Y., He, Y.-F., Wang, Y., & Wang, R.-M. (2013). Study on effective extraction of chicken feather keratins and their films for controlling drug release. *Biomaterials Science*, *1*(5), 528–536.

Yoshimizu, H., Mimura, H., & Ando, I. (1991). I3C CP/MAS NMR Study of the Conformation of Stretched or Heated Low-Sulfur Keratin Protein Films. *Macromolecules*, *24*(4), 862–866.

Yu, Z., Zhang, B., Yu, F., Xu, G., & Song, A. (2012). A real explosion: The requirement of steam explosion pretreatment. *Bioresource Technology*, *121*, 335–341.

Zainal-Abidin, M. H., Hayyan, M., Hayyan, A., & Jayakumar, N. S. (2017). New horizons in the extraction of bioactive compounds using deep eutectic solvents: A review. *Analytica Chimica Acta*, *979*, 1–23.

Zhan, M., & Wool, R. P. (2011). Mechanical Properties of Chicken Feather Fibers Mingjiang. *Polymer Composites*, *32*(6), 937–944.

Zhang, Y., Yang, R., & Zhao, W. (2014). Improving digestibility of feather meal by steam flash explosion. *Journal of Agricultural and Food Chemistry*, *62*(13), 2745–2751.

Zhang, Y., Zhao, W., & Yang, R. (2015). Steam Flash Explosion Assisted Dissolution of Keratin from Feathers. *ACS Sustainable Chemistry and Engineering*, *3*(9), 2036–2042.

Zhao-Tie, L., Ping, S., & Zhong-Wen, L. (2009). Chemically modified chicken feather as sorbent for removing toxic chromium(VI) ions. *Industrial and Engineering Chemistry Research*, *48*(14), 6882–6889.

Zhao, W., Yang, R., Zhang, Y., & Wu, L. (2012). Green Chemistry Sustainable and practical utilization of feather keratin by an innovative physicochemical pretreatment : high density steam flash-explosion.

Zhao, Z., Wang, Y., Li, M., & Yang, R. (2015). High performance N-doped porous activated carbon based on chicken feather for supercapacitors and CO_2 capture. *RSC Advances*, *5*(44), 34803–34811.

Zhu, G., Zhu, X., Fan, Q., & Wan, X. (2011). Raman spectra of amino acids and their aqueous solutions. *Spectrochimica Acta - Part A: Molecular and Biomolecular Spectroscopy*, *78*(3), 1187–1195.

Appendices

Appendix 1. Deconvoluted FTIR spectra.

Appendix 2. Deconvoluted Raman spectra.

Appendix 3. Deconvoluted XRD patterns.

Appendix 4. Deconvoluted NMR spectra.

Appendix 1.

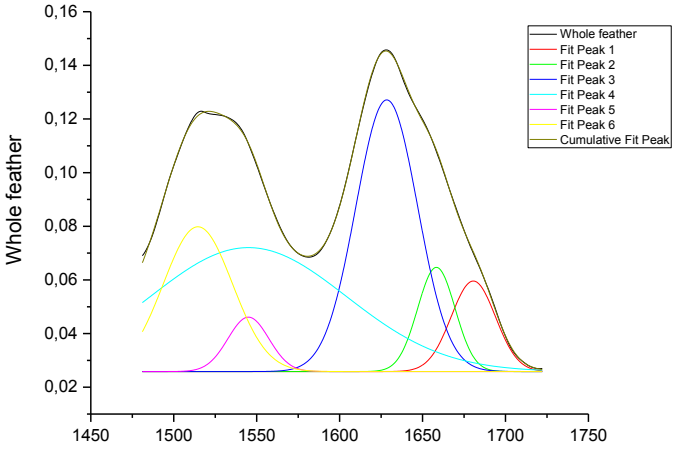

Model	Gaussian					
Equation	y = y0 + A/(w*sqrt(pi/(4*ln(2)))) * exp(-4*ln(2)*(x-xc)^2/w^2)					
Plot	Peak1(Whole feather)	Peak2(Whole feather)	Peak3(Whole feather)	Peak4(Whole feather)	Peak5(Whole feather)	Peak6(Whole feather)
y0	0,02584 ± 3,32285E-4	0,02584 ± 3,32285E-4	0,02584 ± 3,32285E-4	0,02584 ± 3,32285E-4	0,02584 ± 3,32285E-4	0,02584 ± 3,32285E-4
xc	1680,60062 ± 0,80053	1658,33689 ± 0,37191	1628,43625 ± 0,17163	1545,02295 ± 2,71674	1545,01846 ± 0,34115	1514,56637 ± 0,35269
A	1,12948 ± 0,09226	1,09888 ± 0,10195	4,75836 ± 0,17259	6,83711 ± 0,27647	0,62699 ± 0,08215	2,8195 ± 0,18152
w	31,41282 ± 1,003	26,58155 ± 0,76462	43,92826 ± 0,64972	139,01544 ± 8,12485	29,00339 ± 0,99057	49,07702 ± 1,60354
Reduced Chi-Sqr	2,37259E-7					
R-Square(COD)	0,99977					
Adj. R-Square	0,99977					

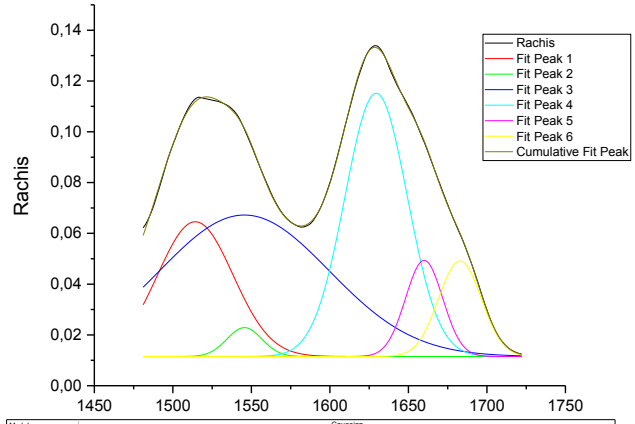

Model	Gaussian					
Equation	y = y0 + A/(w*sqrt(pi/(4*ln(2)))) * exp(-4*ln(2)*(x-xc)^2/w^2)					
Plot	Peak1(Rachis)	Peak2(Rachis)	Peak3(Rachis)	Peak4(Rachis)	Peak5(Rachis)	Peak6(Rachis)
y0	0,01151 ± 2,26931E-4	0,01151 ± 2,26931E-4	0,01151 ± 2,26931E-4	0,01151 ± 2,26931E-4	0,01151 ± 2,26931E-4	0,01151 ± 2,26931E-4
xc	1514,28188 ± 0,36474	1545,54605 ± 0,34597	1545,54605 ± 3,97546	1629,4729 ± 0,19484	1660,01482 ± 0,48742	1682,81523 ± 0,834
A	3,19104 ± 0,4245	0,31624 ± 0,05358	7,53727 ± 0,38545	5,16833 ± 0,19863	1,12363 ± 0,12805	1,28478 ± 0,09902
w	56,49617 ± 2,82762	26,13329 ± 1,2935	127,10597 ± 5,0443	46,84965 ± 0,763	27,89599 ± 0,94684	32,0977 ± 0,98187
Reduced Chi-Sqr	2,5787E-7					
R-Square(COD)	0,99975					
Adj. R-Square	0,99974					

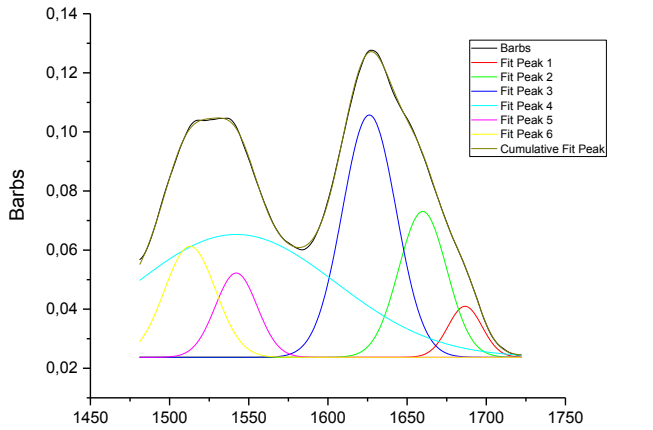

Model	Gaussian					
Equation	y = y0 + A/(w*sqrt(pi/(4*ln(2)))) * exp(-4*ln(2)*(x-xc)^2/w^2)					
Plot	Peak1(Barbs)	Peak2(Barbs)	Peak3(Barbs)	Peak4(Barbs)	Peak5(Barbs)	Peak6(Barbs)
y0	0,02372 ± 4,99803E-4	0,02372 ± 4,99803E-4	0,02372 ± 4,99803E-4	0,02372 ± 4,99803E-4	0,02372 ± 4,99803E-4	0,02372 ± 4,99803E-4
xc	1686,58347 ± 0,5954	1659,88289 ± 0,37844	1628,14988 ± 0,46088	1542,10915 ± 1,9956	1542,09689 ± 0,47431	1512,93461 ± 0,50127
A	0,4648 ± 0,0832	1,8764 ± 0,12957	3,49568 ± 0,2005	6,5707 ± 0,31579	0,94388 ± 0,09009	1,51718 ± 0,07674
w	25,3198 ± 0,917	35,72566 ± 1,64832	40,04927 ± 0,87662	148,51088 ± 10,55673	31,09745 ± 0,88545	37,95013 ± 1,03511
Reduced Chi-Sqr	2,25537E-7					
R-Square(COD)	0,99971					
Adj. R-Square	0,9997					

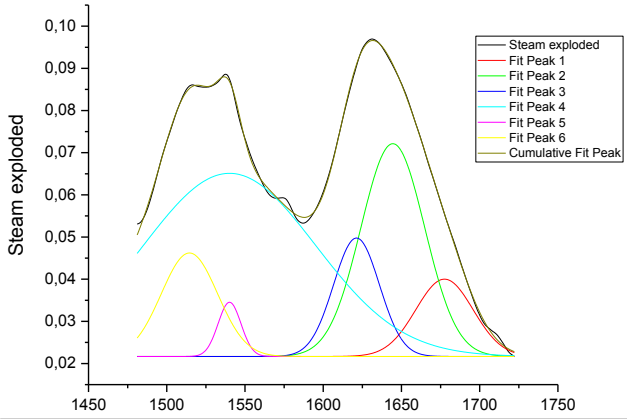

Model	Gaussian					
Equation	y = y0 + A(w*sqrt(pi/(4*ln(2)))) * exp(-4*ln(2)*(x-xc)^2/w^2)					
Plot	Peak1(Steam exploded)	Peak2(Steam exploded)	Peak3(Steam exploded)	Peak4(Steam exploded)	Peak5(Steam exploded)	Peak6(Steam exploded)
y0	0,02168 ± 4,01333E-4	0,02168 ± 4,01333E-4	0,02168 ± 4,01333E-4	0,02168 ± 4,01333E-4	0,02168 ± 4,01333E-4	0,02168 ± 4,01333E-4
xc	1677,49416 ± 7,30818	1644,48519 ± 7,10346	1621,27109 ± 2,07482	1540,12623 ± 2,0268	1540,12623 ± 0,16314	1514,50457 ± 0,30931
A	0,84036 ± 0,64014	2,57718 ± 1,80311	1,03142 ± 1,18203	5,99365 ± 0,1546	0,23537 ± 0,01711	1,10666 ± 0,10078
w	43,06311 ± 4,79057	47,98364 ± 16,69088	34,50467 ± 5,04852	129,65363 ± 4,79337	17,20859 ± 0,53884	42,36993 ± 1,71605
Reduced Chi-Sqr	3,46222E-7					
R-Square(COD)	0,99918					
Adj. R-Square	0,99914					

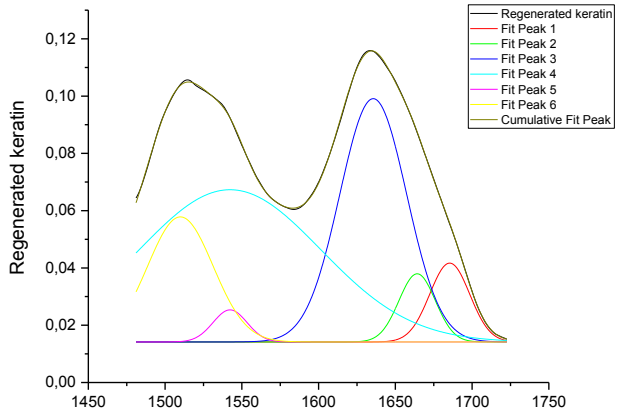

Model	Gaussian					
Equation	y = y0 + A(w*sqrt(pi/(4*ln(2)))) * exp(-4*ln(2)*(x-xc)^2/w^2)					
Plot	Peak1(Regenerated keratin)	Peak2(Regenerated keratin)	Peak3(Regenerated keratin)	Peak4(Regenerated keratin)	Peak5(Regenerated keratin)	Peak6(Regenerated keratin)
y0	0,01416 ± 1,6926E-4	0,01416 ± 1,6926E-4	0,01416 ± 1,6926E-4	0,01416 ± 1,6926E-4	0,01416 ± 1,6926E-4	0,01416 ± 1,6926E-4
xc	1685,42451 ± 0,91801	1664,2145 ± 0,75001	1635,69277 ± 0,22189	1542,31039 ± 1,83891	1542,31005 ± 0,25738	1509,96016 ± 0,16291
A	0,89865 ± 0,07686	0,70764 ± 0,10872	4,94318 ± 0,11678	7,8753 ± 0,21703	0,31656 ± 0,03125	2,33703 ± 0,13797
w	30,86978 ± 0,95161	27,95058 ± 1,15873	51,35544 ± 0,61593	139,20115 ± 3,41459	26,05993 ± 0,78478	50,2859 ± 1,40722
Reduced Chi-Sqr	1,05395E-7					
R-Square(COD)	0,99866					
Adj. R-Square	0,99865					

Appendix 2.

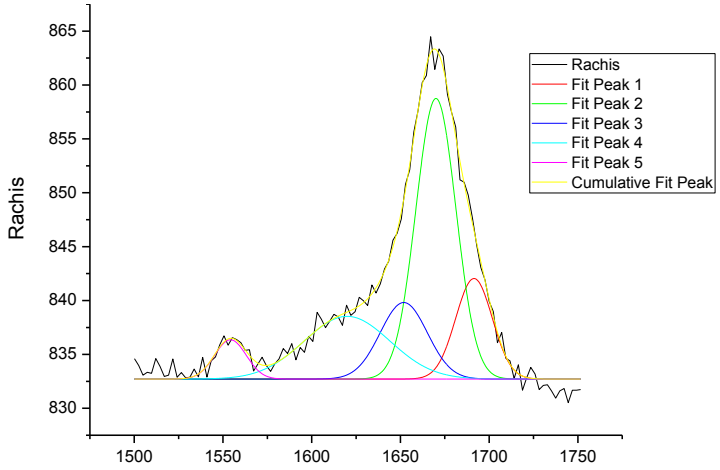

Model	Gaussian				
Equation	y = y0 + A/(w*sqrt(pi/(4*ln(2)))) * exp(-4*ln(2)*(x-xc)^2/w^2)				
Plot	Peak1(Rachis)	Peak2(Rachis)	Peak3(Rachis)	Peak4(Rachis)	Peak5(Rachis)
y0	832,71173 ± 0,16979	832,71173 ± 0,16979	832,71173 ± 0,16979	832,71173 ± 0,16979	832,71173 ± 0,1697
xc	1691,47653 ± 10,331	1670,02488 ± 9,4745	1651,89283 ± 77,5258	1619,93362 ± 23,999	1554,19339 ± 1,413
A	240,95331 ± 335,374	736,36076 ± 1963,48	236,31054 ± 1931,675	352,50722 ± 332,723	81,46577 ± 15,7753
w	24,26037 ± 8,10326	26,56627 ± 17,93612	31,25874 ± 76,51027	56,88342 ± 28,86834	20,99974 ± 3,53524
Reduced Chi-S	0,78196				
R-Square(COD)	0,99085				
Adj. R-Square	0,98935				

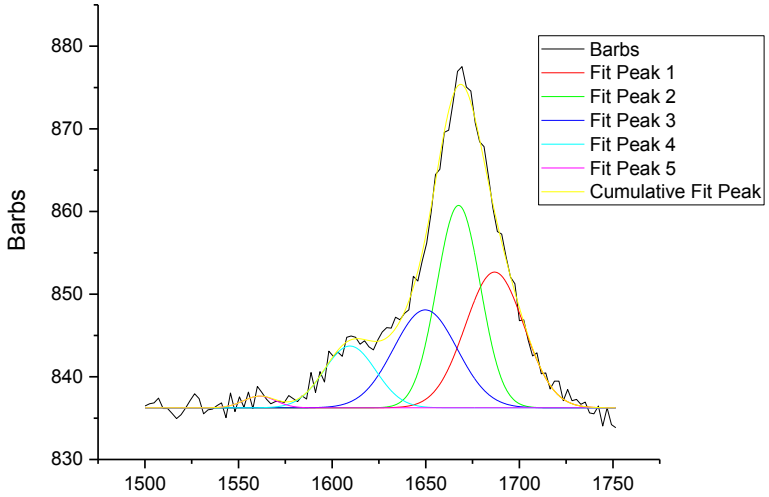

Model	Gaussian				
Equation	y = y0 + A/(w *sqrt(pi/(4*ln(2)))) * exp(-4*ln(2)*(x-xc)^2/w ^2)				
Plot	Peak1(Barbs)	Peak2(Barbs)	Peak3(Barbs)	Peak4(Barbs)	Peak5(Barbs)
y0	836,25084 ± 0,2179	836,25084 ± 0,2179	836,25084 ± 0,2179	836,25084 ± 0,2179	836,25084 ± 0,2179
xc	1686,79247 ± 13,96605	1667,55568 ± 6,21298	1649,78204 ± 115,40457	1609,51218 ± 14,93189	1561,31723 ± 4,01731
A	643,88179 ± 714,14545	713,4609 ± 3460,22956	502,97155 ± 4113,74361	258,00124 ± 364,8835	30,5005 ± 15,46533
w	36,84102 ± 11,67278	27,3725 ± 18,3406	39,88924 ± 157,55822	32,43441 ± 13,70113	20,34327 ± 10,32659
Reduced Chi-Sqr	1,16219				
R-Square(COD)	0,99239				
Adj. R-Square	0,99114				

Appendix 3.

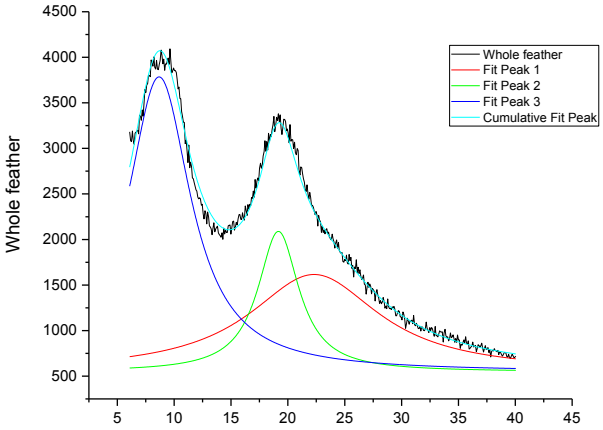

Model	Lorentz		
Equation	y = y0 + (2*A/pi)*(w/(4*(x-xc)^2 + w^2))		
Plot	Peak1(Whole feather)	Peak2(Whole feather)	Peak3(Whole feather)
y0	547,05828 ± 22,07894	547,05828 ± 22,07894	547,05828 ± 22,07894
xc	22,30809 ± 0,4514	19,16836 ± 0,03631	8,6754 ± 0,02144
w	13,94237 ± 0,63373	4,38996 ± 0,28932	6,74753 ± 0,11143
A	23405,86527 ± 2681,35215	10630,70869 ± 1369,22908	34316,96293 ± 644,2875
Reduced Chi-Sqr	6661,86043		
R-Square(COD)	0,99349		
Adj. R-Square	0,99335		

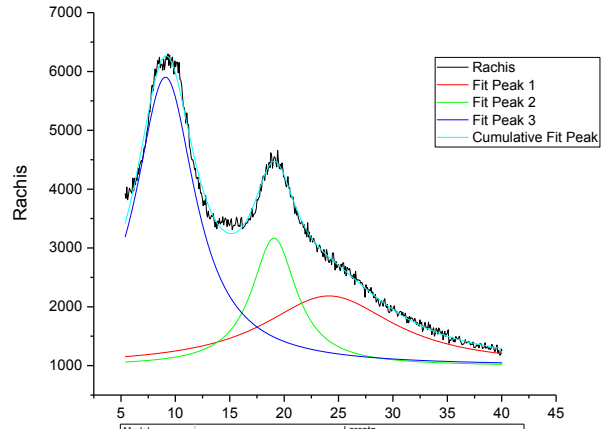

Model	Lorentz		
Equation	y = y0 + (2*A/pi)*(w/(4*(x-xc)^2 + w^2))		
Plot	Peak1(Rachis)	Peak2(Rachis)	Peak3(Rachis)
y0	991,81536 ± 51,86396	991,81536 ± 51,86396	991,81536 ± 51,86396
xc	24,11841 ± 0,61931	19,07116 ± 0,03933	9,0907 ± 0,01856
w	14,80101 ± 1,4415	5,00386 ± 0,29724	6,6662 ± 0,06848
A	27735,35962 ± 5285,851	17091,40496 ± 2008,43	51418,96457 ± 573,050
Reduced Chi-Sq	12796,21028		
R-Square(COD)	0,99367		
Adj. R-Square	0,99353		

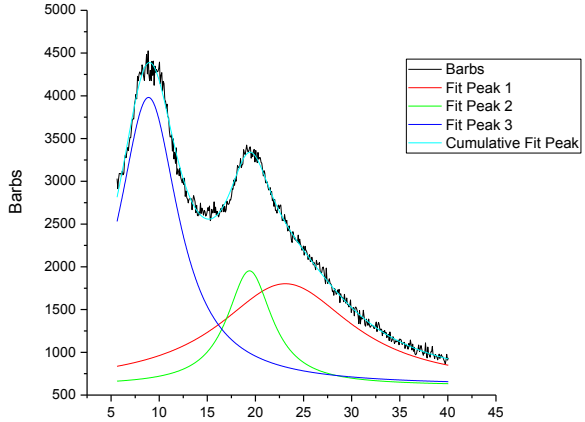

Model	Lorentz		
Equation	y = y0 + (2*A/pi)*(w/(4*(x-xc)^2 + w^2))		
Plot	Peak1(Barbs)	Peak2(Barbs)	Peak3(Barbs)
y0	608,0394 ± 30,31146	608,0394 ± 30,31146	608,0394 ± 30,31146
xc	23,11457 ± 0,59086	19,38154 ± 0,04357	8,88645 ± 0,02198
w	17,02403 ± 0,81749	5,67767 ± 0,42281	7,53292 ± 0,10648
A	31932,28546 ± 4268,83	11996,39218 ± 1972,22	39907,92385 ± 790,99
Reduced Chi-S	4660,73988		
R-Square(COD)	0,99556		
Adj. R-Square	0,99546		

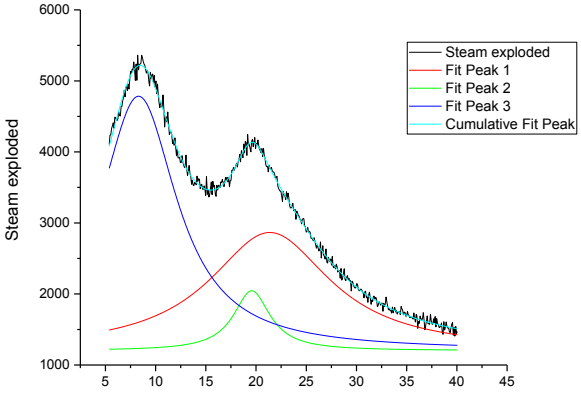

Model	Lorentz		
Equation	y = y0 + (2*A/pi)*(w/(4*(x-xc)^2 + w^2))		
Plot	Peak1(Steam exploded	Peak2(Steam explode	Peak3(Steam explode
y0	1202,29239 ± 17,2484	1202,29239 ± 17,248	1202,29239 ± 17,248
xc	21,36898 ± 0,18925	19,56855 ± 0,05662	8,29826 ± 0,02096
w	14,71088 ± 0,4271	4,42017 ± 0,41045	9,29157 ± 0,12484
A	38434,71795 ± 1782,0	5855,78393 ± 1084,1	52277,24665 ± 837,3
Reduced Chi-	3949,34453		
R-Square(CO	0,99708		
Adj. R-Square	0,99702		

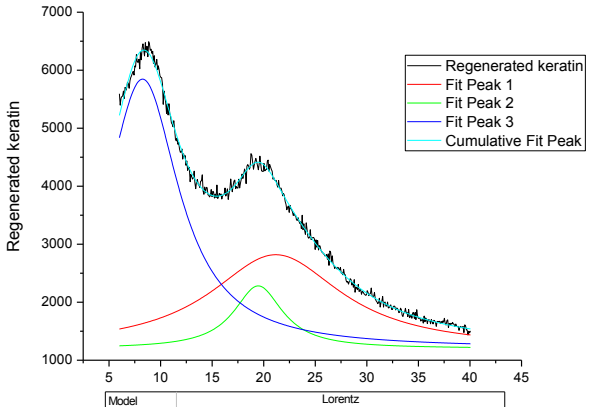

Model	Lorentz		
Equation	y = y0 + (2*A/pi)*(w/(4*(x-xc)^2 + w^2))		
Plot	Peak1(Regenerated	Peak2(Regenerated	Peak3(Regenerated
y0	1201,13439 ± 24,618	1201,13439 ± 24,618	1201,13439 ± 24,618
xc	21,17473 ± 0,36686	19,47171 ± 0,08166	8,25915 ± 0,02047
w	15,55653 ± 0,78253	5,75868 ± 0,68839	8,54226 ± 0,13528
A	39533,4471 ± 3717,6	9773,8554 ± 2833,74	62325,42017 ± 1241,
Reduced Chi	6089,19336		
R-Square(C	0,99717		
Adj. R-Squar	0,99711		

Appendix 4.

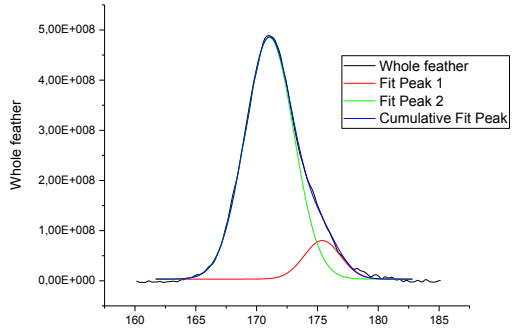

Model	Gaussian	
Equation	y = y0 + A/(w*sqrt(pi/(4*ln(2)))) * exp(-4*ln(2)*(x-xc)^2/w^2	
Plot	Peak1(Whole feather)	Peak2(Whole feather)
y0	3,39438E6 ± 642781,499	3,39438E6 ± 642781,499
xc	175,39683 ± 0,07668	171,04739 ± 0,01606
A	2,87944E8 ± 1,67651E7	2,42694E9 ± 1,84133E7
w	3,52274 ± 0,1323	4,73188 ± 0,03146
Reduced Chi-Sqr	2,26242E13	
R-Square(COD)	0,99916	
Adj. R-Square	0,99912	

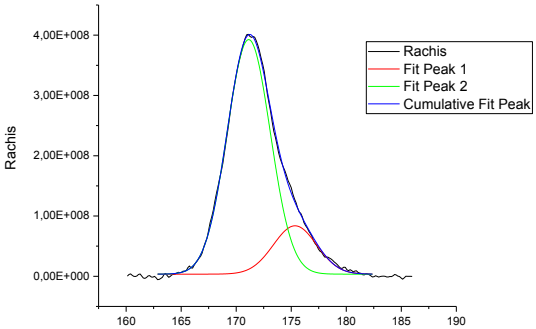

Model	Gaussian	
Equation	y = y0 + A/(w*sqrt(pi/(4*ln(2)))) * exp(-4*ln(2)*(x-	
Plot	Peak1(Rachis)	Peak2(Rachis)
y0	3,56143E6 ± 694071,6	3,56143E6 ± 694071,6
xc	175,34581 ± 0,16792	171,13725 ± 0,03438
A	3,95351E8 ± 3,50458E	1,90959E9 ± 3,50663E
w	4,63144 ± 0,22238	4,61117 ± 0,0455
Reduced Chi-	1,74216E13	
R-Square(CO	0,99906	
Adj. R-Square	0,99902	

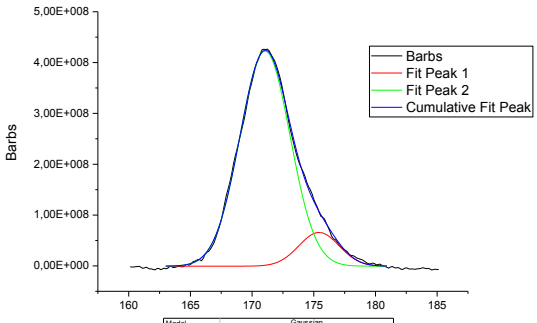

Model	Gaussian	
Equation	y = y0 + A/(w*sqrt(pi/(4*ln(2)))) * exp(-4*ln(2)*(x-xc	
Plot	Peak1(Barbs)	Peak2(Barbs)
y0	-542930,1704 ± 885893, 94708	-542930,1704 ± 885893, 94708
xc	175,42432 ± 0,11619	171,05105 ± 0,02265
A	2,7068E8 ± 2,14588E7	2,15127E9 ± 2,35036E7
w	3,83378 ± 0,18483	4,77704 ± 0,04123
Reduced Chi-S	2,34891E13	
R-Square(COD)	0,99893	
Adj. R-Square	0,99888	

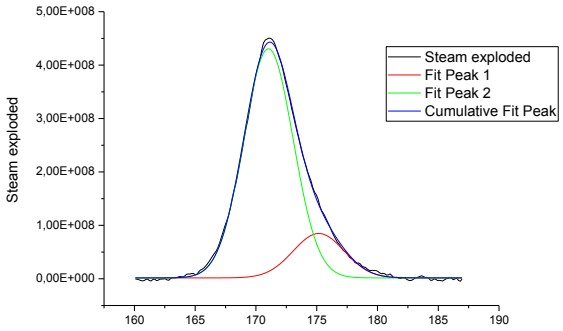

Model	Gaussian	
Equation	y = y0 + A/(w*sqrt(pi/(4*ln(2)))) * exp(-4*ln(2)*(x-xc)^2/w^2	
Plot	Peak1(Steam exploded)	Peak2(Steam exploded)
y0	1,7193E6 ± 468017,5007	1,7193E6 ± 468017,5007
xc	175,16617 ± 0,22806	171,02492 ± 0,04184
A	4,37068E8 ± 5,01277E7	2,18498E9 ± 4,99662E7
w	4,94296 ± 0,26878	4,78679 ± 0,04811
Reduced Chi-Sqr	1,81648E13	
R-Square(COD)	0,99911	
Adj. R-Square	0,99908	

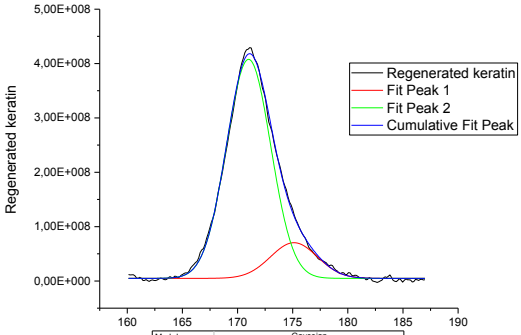

Model	Gaussian	
Equation	y = y0 + A/(w*sqrt(pi/(4*ln(2)))) * exp(-4*ln(2)*(x-xc	
Plot	Peak1(Regenerated ker	Peak2(Regenerated ker
y0	4,85254E6 ± 532516,7	4,85254E6 ± 532516,7
xc	175,11519 ± 0,33812	171,00032 ± 0,05003
A	3,48488E8 ± 5,78678E	2,02453E9 ± 5,75515E
w	4,99165 ± 0,40038	4,72116 ± 0,0568
Reduced Chi-	2,35919E13	
R-Square(CO	0,99866	
Adj. R-Square	0,99861	